I. THE BROADENING OF THE RESONANCE LINES OF RUBIDIUM UNDER DIFFERENT HOMOGENEOUS PRESSURES OF ITS OWN VAPOR

II. THE BROADENING, ASYMMETRY AND SHIFT OF RUBIDIUM RESONANCE LINES UNDER HOMOGENEOUS PRESSURES OF HELIUM AND ARGON UP TO 100 ATMOSPHERES

Thesis by

Shang-yi Ch'en

In partial Fulfillment of the Requirements

for the Degree of Doctor of Philosophy

California Institute of Technology

Pasadena, California

1940

THESIS I

THE BROADENING OF THE RESONANCE LINES OF RUBIDIUM UNDER DIFFERENT HOMOGENEOUS PRESSURES OF ITS OWN VAPOR

A B S T R A C T

The broadening of the resonance lines of rubidium in absorption under pressures up to 152 mm. Hg of its own homogeneous vapor was studied by means of a 21-foot grating. Under pressures below 1 mm. Hg the broadening of the lines was very symmetrical and the line contours could be described by the dispersion formula, but when the pressure was high the lines exhibited asymmetrical broadening. The $^2P_{\frac{1}{2}}$ component showed red, while the $^2P_{3/2}$ component showed violet asymmetry. The broadening of the shorter wavelength component is greater than that of the longer wavelength component. Both lines showed the proportionality of the width with N. The experimental half width is greater than that predicted by Prof. Houston's theory by a factor of 3. 1½

A narrow band was observed near the shorter wavelength side of the $^2P_{\frac{1}{2}}$ component and a similar one near the longer wavelength side of the $^2P_{3/2}$ component.

C O N T E N T S

THE BROADENING OF THE RESONANCE LINES OF Rb UNDER DIFFERENT PRESSURES OF ITS OWN VAPOR

I. INTRODUCTION

Previous experimental determinations of the broadening of spectral lines due to the influence of the atoms of the same kind (resonance broadening) were found to be erroneous because a certain amount of foreign gas was generally present in the absorption tube[1]. The purpose of introducing foreign gas into the absorption tube was to prevent too quick distillation of the absorbing substances to its cooler part; the windows had to be kept cold to prevent them from being attacked by the alkali vapors. Otherwise, the broadening could be studied only at very low pressures[2] (say, at 10^{-3} mm. Hg) for the absorption tube could be heated only to such a temperature that the effect of the vapor on the windows did take place.

The above experimental difficulity has been eliminated after the new corrosion-resistant MgO windows have been developed[3]. Also with the help of the M_gO windows we can get a homogeneous absorbing vapor column of well determined thickness; thus it is feasible to determine the absolute absorption coefficient.

---

(1) G. R. Harrison, Phys. Rev. 25, 768, 1925;
Harrison and J. C. Slater, Phys. Rev. 26, 176, 1925;
B. Trumpy, Zeits. f. Physik 34, 715, 1925; 40, 594, 1926.
(2) R. Minkowski, Z. f. Physik, 36, 839, 1926;
W. Schutz, Z. f. Physik, 45, 30, 1927;
S. A. Korff, Astrophys. J. 76, 124, 1932; Phys. Rev. 38, 477, 1931;
W. Weingeroff, Z. f. Physik, 67, 679, 1931;
(3) J. Strong and R. T. Brice, J. O. S. A. 25, 207, 1935.

Hughes and Lloyd[4] employed the M_gO windows to observe the broadening of K resonance lines. Due to the small separation of the components of the K resonance lines (34Å) and due to certain experimental difficulities they had not yet overcome, the broadening of the lines was studied for pressures only up to 20 mm. Hg.

The resonance broadening has been investigated theoretically by Prof. Houston[5]. His theoretical results are ~~ten~~ five times too small in comparison with the experimental ones, a discrepancy which is too much beyond the experimental error.

In the present research the corresponding problem for rubidium was studied. With further improvement in making the absorption tube and with the help of much bigger separation of the components of the rubidium resonance lines (147 Å) observations for pressures up to 152 mm. Hg. were made. More new results were obtained to call for further theoretical considerations.

---

(4) Hughes & Lloyd, Phys. Rev. 52, 1215, 1937.

(5) W. V. Houston, Phys. Rev. 54, 884, 1938.

II. THEORY

Detailed review of the theories of the pressure broadening of spectral lines can be found in several review articles[6].

Essentially the process of broadening of a spectral line can be divided into two main parts: I. Broadening when there are no external disturbers; this broadening process will be independent of the density of the gas in which absorption takes place. II. Broadening due to external disturbances of neighbouring atoms; this broadening will depend strongly on the density.

The first part includes two well known processes: (a) natural damping, (b) Doppler effect. Classically the natural width is due to a vibrating charge continually damping by the radiation of energy. The half width is approximately independent of the wavelength and is of the order of 10^{-4} A which is negligibly small in the present research. Doppler broadening is due to random motions of the absorbing atoms. The effect decreases with wavelength and has no apparent shift of the central maximum of the line. By assuming Maxwellian distribution of the velocities it is easy to show that the intensity distribution decreases exponentially with the frequency difference from the central maximum. In the present

---

(6) V. Weisskopf, Phys. Zeits. 34, 1, 1933.
H. Margenau and W. W. Watson, Rev. Mod. Phys. 8, 22, 1936.
P. Schulz, Phys. Zeits. 39, 412, 1938.
P. E. Lloyd's unpublished Ph. D. thesis, General Library, Calif. Inst. of Tech. 1937.

experiment the line width was calculated from the wings, the Doppler broadening was naturally neglected.

The broadening underlying the effect of the second part can again be divided into two classes (a) the influence of the atoms of the same kind (b) that of a foreign atom.

The broadening in the first class is mainly due to the resonance forces and that in the second class is chiefly due to the van der Waals forces. When an excited atom interacts with a normal one of the same kind at a rather large internuclear distance with a potential of force proportional to $1/R^3$, the effect is said to be due to "resonance forces". Approximately[7] the resonance perturbation energies are given as

$$E = (e^2 hf / 8\pi^2 m \nu_o) (1/R^3) \qquad (1)$$

where m is the magnetic quantum number of the excited atom and f is the oscillator strength of the transition of natural frequency ν_0. For the broadening due to the van der Waals forces the corresponding equation can be written as

$$E = - Ch / R^6 \qquad (2)$$

where C is a constant of the transition. Although the van der Waals forces in the case of metallic atoms are large, they are small in comparison to the resonance forces.

The maximum of the intensity distribution will correspond to the most probable perturbation value. At moderate

---

(7) Formula (1) is proper at small pressures i.e. when only a single perturbing atom was considered; the simultaneous action of several perturbers being ignored.
See H. Margenau and W. W. Watson, Rev. Mod. Phys. 8, 22, 1936.

pressures the intensity distribution will follow the resonance perturbations because of slower decay with the distance of (1) in comparison with (2). The region can be described by Lorentz's theory. A correction in the formula for the optical mean free path produces a reduction of the values used for the optical collision radii. At higher pressures, i.e. for the large frequency changes of the highly broadened lines the probability of sufficient close multiple approaches is small. The influence of a single atom is predominant. So the wings of the line will take an asymmetrical extension according to the contribution of the van der Waals interactions.

For an analytical discussion of the theoretical part of the problem the reader can best be referred to P. E. Lloyd's thesis[8], to avoid repetition. All the theories dealing with effect of pressure broadening are different points of view of treating the same problem. They might be supposed to be equivalent or different approximations to the complete treatment for they all lead to the same dispersion formula though with different interpretations as to the half-width. Prof. Houston[5] pointed out that there are in general three principal methods of calculating the collision broadening which are merely three approximations to the exact quantum mechanical treatment.

Obviously in the present research there should be no worry about the broading due to Stark effect for no charged particles were present in the absorption tube.

---

(8) Obtainable from the general library of Calif. Inst. of Tech. Pasadena.

III. EXPERIMENTAL

The experimental arrangement was essentially the same as that used by Dr. Lloyd, so many points will be but briefly discussed. The rubidium vapor was evaporized in an absorption tube which was sealed in a vacuum furnace whose temperature could be controlled and measured. The broadened absorption lines of rubidium were registered by means of a 21-foot grating spectrograph of Rowland mounting with tungsten filament incandescent lamp as light source.

The rubidium metal was prepared by reducing very pure rubidium chloride with metallic calcium. It was then redistilled properly to remove as much as possible any impurities such as oxides, and was sealed in small pyrex tubes of convenient size.

The absorption tube was made of copper with 1.5 cm inside diameter and M_gO windows on both ends. Three tube lengths were employed viz. 15, 7.5, 0.2 cm. For the two longer tubes both ends were cut into sharp edged rings, so they could be made vacuum tight by pressing the sharp rings against the surface of the M_gO windows. The construction of the short tube is shown in Fig. 1. The tube was made of steel. The Rubidium

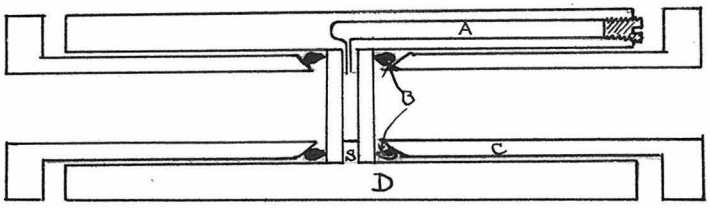

Fig. 1. The 2 mm. long absorption tube

tube was placed inside the hole A whose end was closed by a copper tap screw whose coefficient of expansion was higher than that of the steel so the hole was always tightly closed throughout the experiment. B was a copper ring which worked as a gasket when the tube C was compressed on to the tube D at high temperatures. The copper ring was of course too hard, but it did not react with rubidium to produce almalgan as did aluminum[9]. In this case the length of the absorption tube could also be easily determined because the latter was the thickness of the section S.

The tungsten filament lamp was built with a glass bulb 13 cm in diameter with a glass plug having ground joint to support the filament, and a glass window waxed to the end of the cylinder which projects about 20 cm from the bulb to prevent the vaporized tungsten from depositing on it. The tungsten filament of about 1 mm. in diameter and 2.5 cm long was supported by two nickel electrodes with two small holes at their ends. The latter were screwed into the copper rods attached to a glass plug. After the bulb was evacuated an 80 ampere current was drawn through the filament giving a very intense and constant light source at a temperature of about 3400 K. It served to produce a continuous background of the absorption spectrum with fairly uniform intensity distribution about the

---

(9) Aluminium ring was tried. When the tube was heated to 300 C or higher, a silvery liquid almalgan of rubidium and aluminium appeared in big amount giving no more rubidium absorbing lines.

region of the rubidium resonance lines. The dimensions of the filament were designed to fill the slit of the spectrograph. The life of the filament depended greatly on the vacuum of the bulb, and was about 8 hours. The filament could be replaced within 10 minutes.

The furnace consisted of a heating element placed in a vacuum tight enclosure. The heating element was made of a porcelain tube wound by molybdeum wire with double layers. By regulating the amount of current supplied to each layer a uniform temperature of about 20 cm. long was used to heat the absorption tube. With the D. C. generators in West Bridge Laboratory using the voltage regulation, the temperature of the furnace could be maintained very constant. The constancy of the temperature of the furnace depended not only on the electrical input but also on the vacuum of the furnace. When the vacuum of the furnace was decreased more heat would be conducted away resulting in a lowering of the temperature of the absorption tube. For every exposure the temperature was kept constant within 1° C as indicated by the chromel- alumel thermocouple. The thermocouple was very carefully calibrated "in situ" using tin, lead and zinc.

With the help of two convex lenses the light from the incandescent lamp was brought to pass through the absorption tube and to form an image of the tungsten filament lamp on the slit of the spectrograph. The 21-foot grating had 14500 lines per inch and had an area 5 X 12 $cm.^2$ The resolving power was about 70,000 and the dispersion was 2.64 A/mm. for the first order.

First order spectrum was used throughout using Wratten F-filter to cut out all the higher orders. Eastman Kodak type I-R plates hypersensitized with amonia hydroxide were used. The plate was calibrated by means of two stepweakeners mounted just before the plate on both sides of the absorption lines so that the absorption lines and the density markings could be recorded at once.

The stepweakeners were made from a high contract photographic plate, the density values of which were carefully determined by a sensitometer and by photographic method. The transmission of the stepweakner did not vary appreciably with the wavelength over the range required because practically the same densitometer readings were obtained when the light of the densitometer lantern was first filtered by the F-filter and water then by the D-filter and water.

During experiment each time the absorption tube was cleaned by long pumping and heating. Then metallic rubidium was introduced into the absorption tube in a currentof nitrogen gas. The absorption cell was evacuated immediately. The absorption cell was then sealed off by pressing the M_gO windows against the end of the tube. Finally it was ready to heat. Normally it took about 7 hours to heat the tube to a steady temperature. The absorption tube was set in alignment with the light source and the slit of the spectrograph. Then the newly sensitized photographic plate was mounted. During each exposure the thermocouple readings were taken every hour. In

case the temperature was changed by 2 degrees or more the plate was discarded. The slit of the spectrograph was first set to 20 μ. When the temperature of the tube was raised the absorption lines were considerably broadened a wider slit was used (say 60 μ) to shorten the time of exposure. The plate was carefully developed by Eastman Kodak formula D-19 developer with gentle brushing by camel hair brush.

The chief experimental difficulties were the leakage of the absorption tube at high temperatures and the deposit of the alkali metal on the windows. The former difficulty was especially bad when the tube was made very short (2 mm.). The experiment was repeated eight times before the tube was made completely air tight and served to give the final spectrogram of the broadened rubidium lines at a temperature of 556° C. (pressure 152 (?)[10] mm. Hg).

---

(10) Obtained by too far extrapolation from the vapor pressure formula (11).

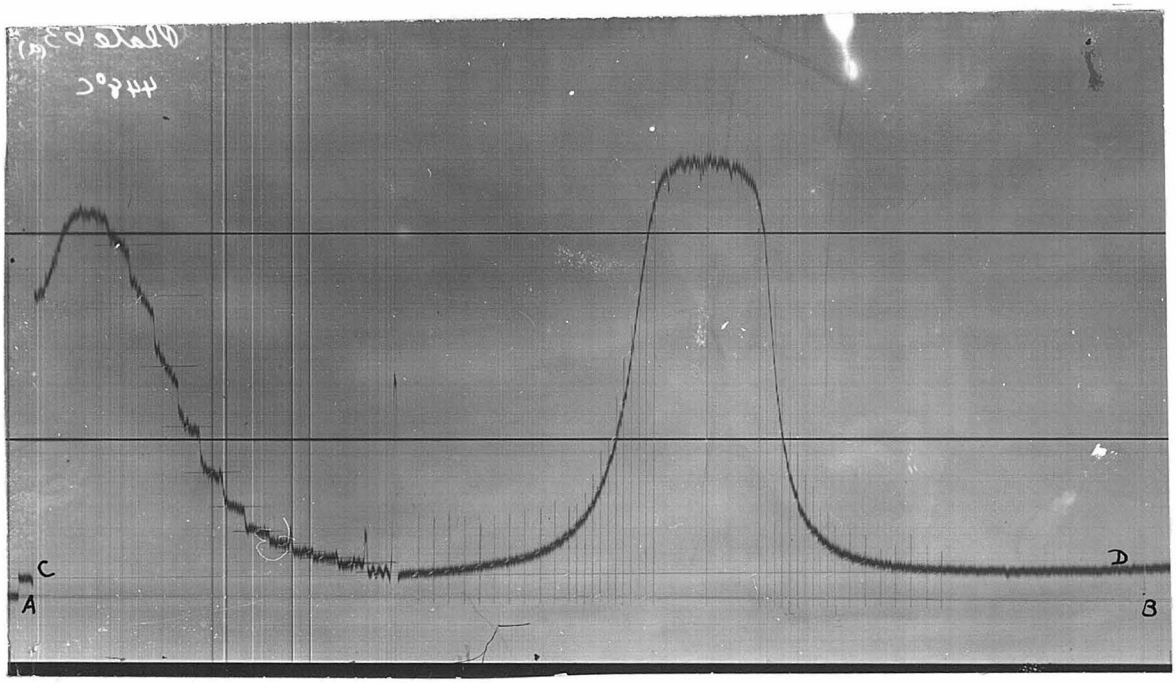

Fig. 2 A sample microphotometer curve

IV. REDUCTION OF OBSERVATIONS

The line contour was traced by a Krüss microphotometer[11]. The magnification 39.8 : 1 was used for rather narrow lines but when the line was very broad 6:1 or 2:1 ratios were set. The size of the microphotometer plate was 9 X 24 cm^2. The microphotometer was always adjusted so that it gave a large deflection with greatest resolving power. In measuring the deflections of the microphotometer traces they were printed very carefully on a paper[12]. Fine parallel lines were drawn to divide the line contour evenly into strips. A sample picture is shown in Fig. 2. A zero line AB was drawn from the deflection on both sides of the microphotometer trace. The deflection of the microphotometer trace could be measured accordingly along the lines. The microphotometer deflections should be corrected with great care for the intensity variation of the background which was due to the variation of the sensitivity of the photographic plate with the wavelength and due to the slight difference of the intensity distribution of the light source in that small range of the spectrum. A spectrum was taken without the step-

---

(11) The microphotometer was located in Room 14A Astrophysics Building, Cal. Tech.

(12) Of course some errors due to the nonuniform contraction throughout the whole area of the bromide paper and the limitation of the accuracy of the pencil lines (accurate within .1 or .2 mm.) will be introduced. But this error will not be appreciable in comparason with those inherent in the irregularities of the microphotometer deflections, in the approximation of the corrections of the calibration curve due to wavelength sensitivity of the background, and in the uncertainty in getting the mean deflections of the respective steps of the stepweakener.

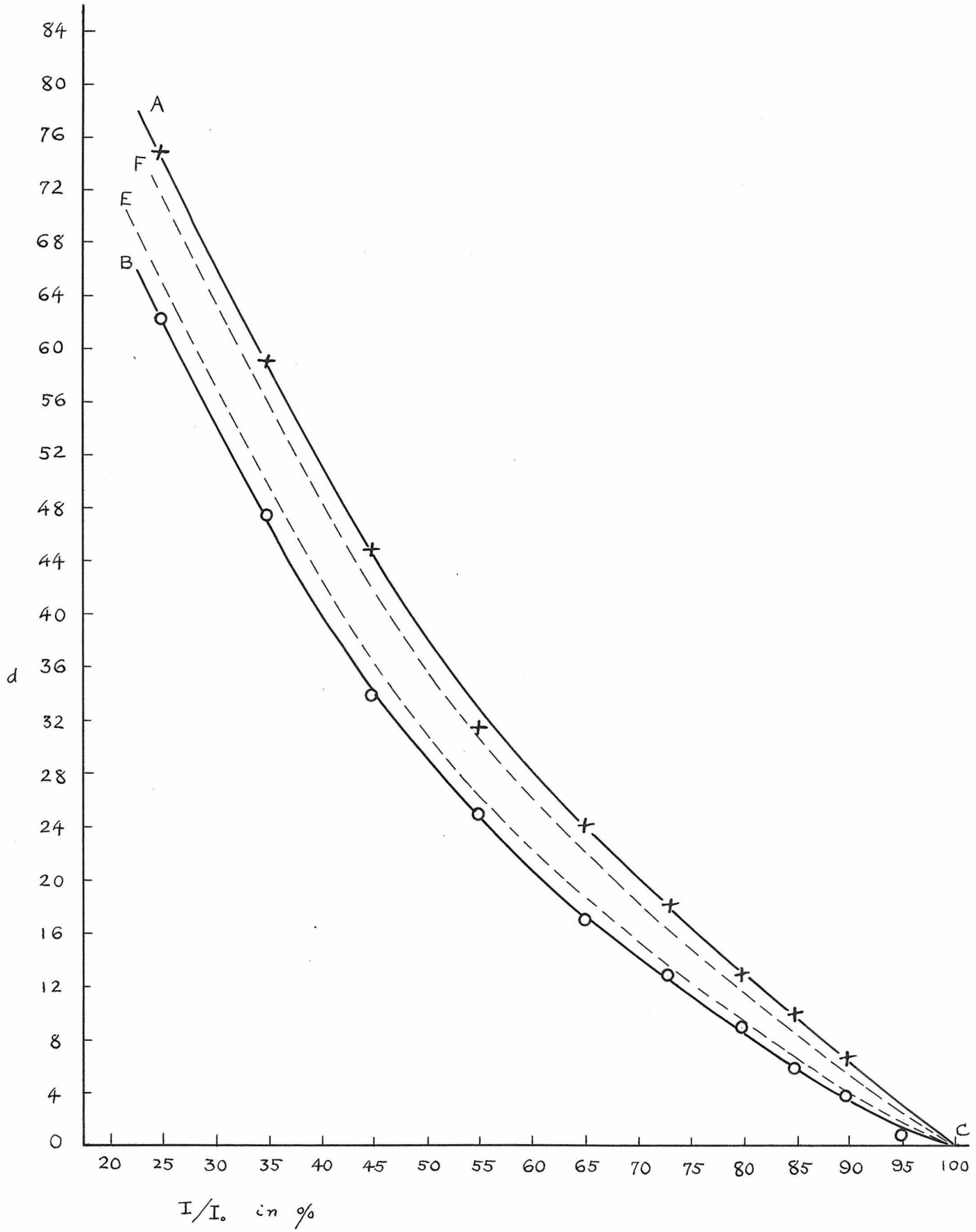
84
80
76
72
68
64
60
56
52
48
44
40
36
32
28
24
20
16
12
8
4
0
d
A
F
E
B
C
20
25
30
35
40
45
50
55
60
65
70
75
80
85
90
95
100
I/I₀ in %

Fig. 3

weakener and absorbing column in position. The microphotometer trace of the background was approximately a straight line indicating that the slope of the resultant of the curves of wavelength sensitivity curve of the plate and the intensity distribution of the background is practically uniform in that small frequency interval.

So in determining the absorption coefficient of the line contours the microphotometer deflection d_1 measured from the zero line AB should be substracted from the height d_0 measured from the zero line AB to the background line CD. The net height d (or better call it "true height") of the microphotometer deflection is actually the deflection caused by the absorption of the alkaline vapor or the stepweakeners.

In this way the calibration curves for each plate were obtained from the stepweakener marks. The two calibration curves obtained from the two stepweakeners in their respective regions of the spectrum should indeed be different on account of the difference of intensity of the background and the wavelength sensitivity of the plate. To the first approximation the variation within the small spectral region could be regarded as linear. So the corrected calibration curves for the region corresponding to the absorption lines were found by interpolation. Fig. 3 shows the sample curves for plate No. 34.

The half-width of the line was determined by the help of the dispersion formula:

$$\alpha x = \frac{\rho \gamma/2\pi}{(\delta\lambda)^2 + (\gamma/2)^2} \qquad (3)$$

where αx is the absorption coefficient = $2.3 \log_{10} I_o/I$

x, the length of the absorption column

ρ, area under the absorption curve

$$= \int_{-\infty}^{+\infty} \alpha x \, d(\delta\lambda) = \frac{\pi e^2 \lambda_o^2}{mc^2} Nfx$$

γ = the half-width

$\delta\lambda = \lambda - \lambda_o$

λ_o being the wavelength of the central maximum

The absorption constant is a function of wavelength and is dependent mainly on the number of atoms per cc. in the absorption tube. So far for a given concentration of the adsorbing atoms in the absorption tube and for a given line, the area under the absorption coefficient curve is a constant, and γ is a constant. So formula (3) can be written as

$$\alpha x = \frac{C_1}{(\delta\lambda)^2 + C_2} \qquad (4)$$

where C_1 and C_2 are constants.

Since $$\frac{I}{I_o} = e^{-\alpha x} = e^{-\frac{C_1}{(\delta\lambda)^2 + C_2}} \qquad (5)$$

Solve for $(\delta\lambda)^2$

$$(\delta\lambda)^2 = C_1\left(\frac{\log_{10} e}{\log_{10} \frac{I_o}{I}} - \frac{C_2}{C_1}\right) \qquad (6)$$

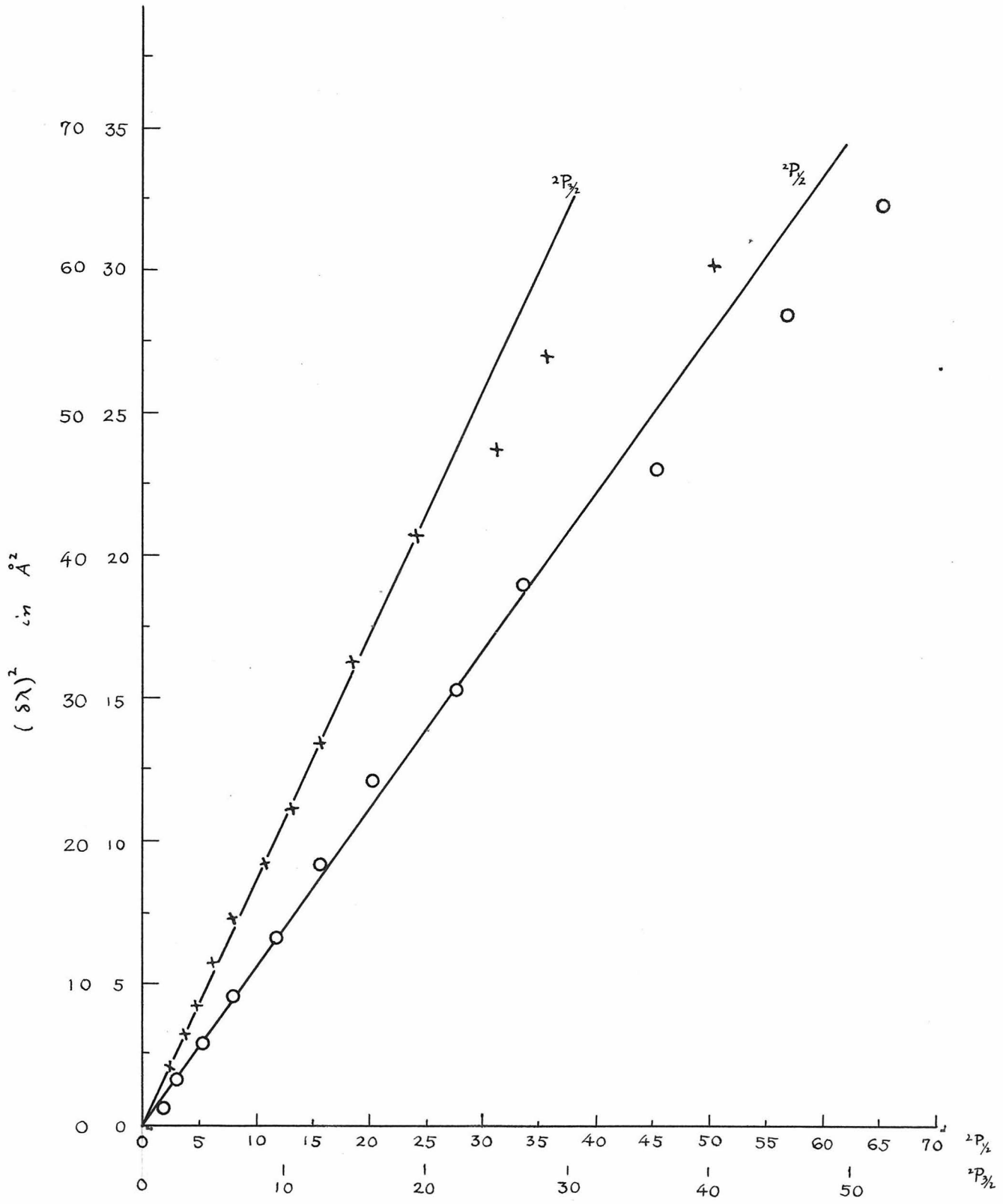

Fig. 4 The $(\delta\lambda)^2$ vs. $(\log_{10}L/I)^{-1}$ curve for Plate No. 34

So a plot with $(\delta\lambda)^2$ as ordinate against $(\log_{10}\frac{I_0}{I})^{-1}$ as abscissa, is a straight line with slope $C = \log_{10} e\, C_1$ and intercept C_2. C_2 was practically nil showing that the central maximum of the line exhibited nearly complete absorption. Fig. 4 is a sample curve for plate No. 34.

So $C = (d\lambda)^2 \log_{10}\frac{I_0}{I}$ can be found experimentally. While theoretically,

$$C = \log_{10} e\ C_1 = (d\lambda)^2 \times \log_{10}\frac{I_0}{I}$$

$$= \frac{\rho\gamma}{2\pi}\Big/(\delta\lambda)^2 (\delta\lambda)^2 \log_{10} e = \frac{\rho\gamma}{2\pi}\log_{10} e \qquad (7)$$

Or
$$\rho\gamma = 2\pi C \Big/ \log_{10} e \qquad (8)$$

where ρ = area under the absorption coefficient curve

$$= \int_{-\infty}^{+\infty} \alpha x\, d(\delta\lambda)$$

$$= \frac{\pi e^2 \lambda_0^2}{mc^2} Nfx \qquad (9)$$

where N denotes the number of atoms per cc.

f, the oscillator strength of the transition of natural frequency corresponding to λ_0

and x, the length of the absorption column

So γ can be calculated theoretically giving

$$\gamma = 2\pi C \Big/ (\rho \log_{10} e) \qquad (10)$$

Thus the final aim of the finding from the spectrograms was the best determination of the value of C.

Two other quantities had to be determined in addition to the value of C — the length of the absorption column and the temperature of the absorption tube. There was no difficulty in measuring the tube-lengths. The tube lengths varied from 15.06 cm. to 0.196 cm., a factor of 76.8.

The temperature of the absorption tube was the measure of the saturated vapor pressure of rubidium in the absorbing column. The temperature vs. vapor pressure curve for rubidium has been studied by Scott, Killian and others[13]. From Critical Tables

$$\log_{10} p = -52.23 \times 76/T + 6.976 \qquad (11)$$

where p is the vapor pressure of rubidium in mm. Hg;

T the absolute temperature.

The formula was used over the entire temperature range although it was set to cover the range 250-370° C only.

The number of atoms per cc. is

$$N = 9.70 \times 10^{18}\ p/T \qquad (12)$$

The temperature covered 136° C - 556° C corresponding to pressures from .0019 to 151.4 mm. Hg., a factor of about 80000 in N.

---

(13) Ruff & Johannsen, Ber. d. deuts. Chem. Ges. 38, 360, (1905)
Hackspill, Comptes Rendus, 154, 877, 1912.
Scott, Phil. Mag. 47, 32, 1924.
Egerton, Phil. Mag. 48, 1048, 1924
Killian, Phys. Rev. 27, 578, 1926.

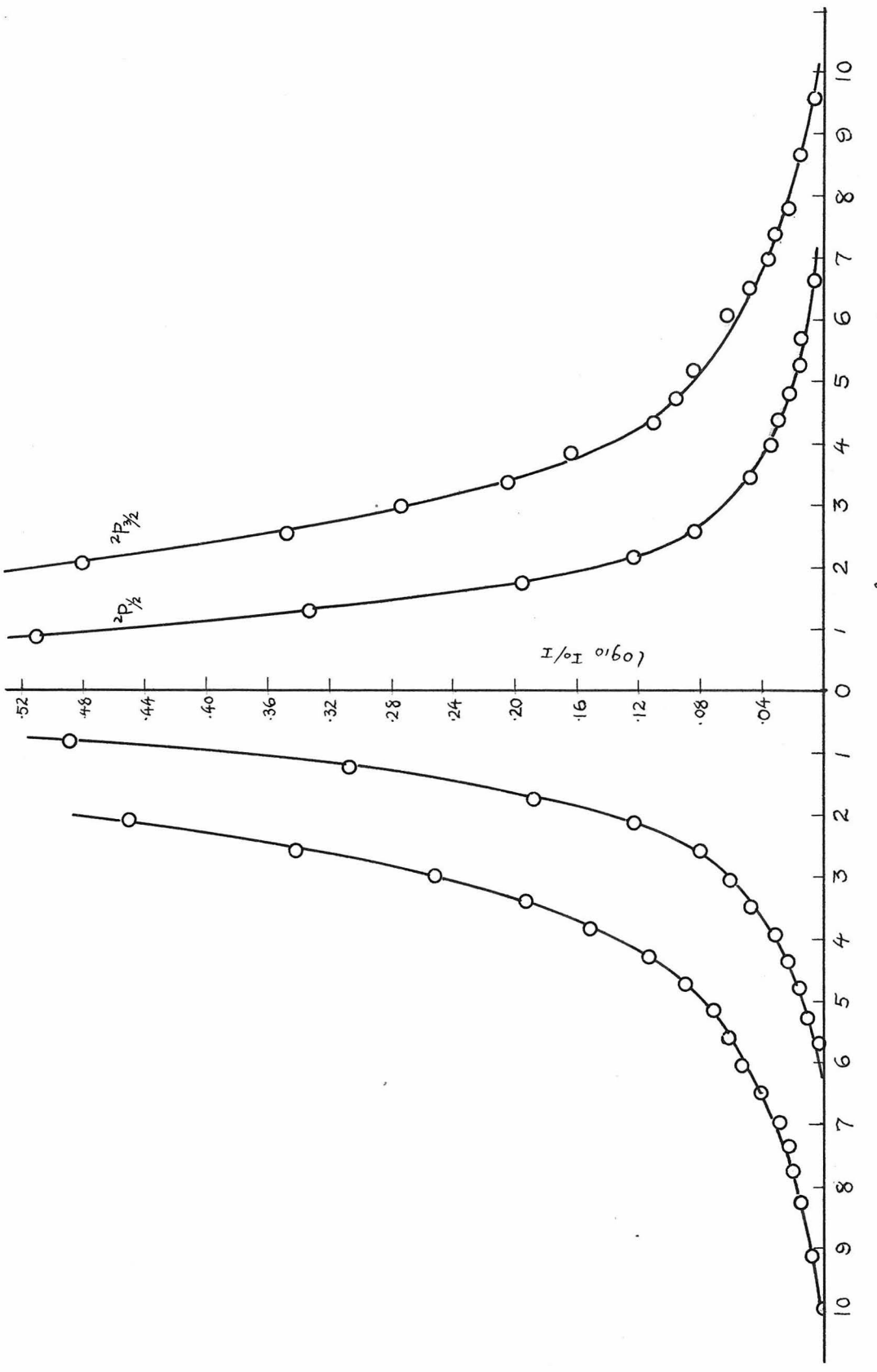

Fig. 5 The symmetrical line contours of Rb resonance lines for Plate No. 34 ($T = 563°K$ $p = 0.983$ m.m. Hg $x = 0.2$ cm.)

V. RESULTS AND DISCUSSION

Following the methods of calculation discussed in the above chapter, all spectrograms were analysed. As shown in Fig. 5, the lines were very symmetrically broadened when the vapor pressure was below about 1 mm. Hg. But for plates taken when the temperature of the tube was raised to about 290° c or more the lines exhibit more and more asymmetrical broadening, and a shadow of absorption was observed near the broadened line components. All results are presented under two items, viz. the broadening when the vapor pressure was low; and that when the vapor pressure was high as follows:

A. Observations of the Line Broadening under Low Pressures.

(a) Test of the formulas of resonance broadening

According to Lorentz collision broadening[14] the half width

$$\gamma = (\lambda_0^2 \rho_0^2 \bar{v}/c) N \qquad (13)$$

where ρ_0 is the optical collision diameter.

For the modified Lorentz theory[15]

$$\gamma = \left(\frac{e^2 \lambda_0^3}{2\pi mc^2}\right) Nf \qquad (14)$$

For Margenau and Watson's derivation[16]

$$\gamma = \left(\frac{e^2 \lambda_0^3}{6\ mc^2}\right) Nf \qquad (15)$$

---

(14) H. A. Lorentz, Proc. Amst. Acad. 8, 591, 1906.
(15) A. Kuhn, Phil. Mag. 48, 987, 1937.
(16) W. W. Watson & H. Margenau, Rev. Mod. Phys. 8, 22, 1936.

TABLE

Plate No.	T °K	p mm. Hg.	N	C_1
	Tube length = 15.06 cms.			
A2	409	1.866×10^{-3}	4.42×10^{13}	2.82×10^{-19}
A3	445	1.14×10^{-2}	2.44×10^{14}	4.76×10^{-18}
	Tube length = 7.50 cms.			
B2	454	1.35×10^{-2}	2.88×10^{14}	3.28×10^{-18}
B4	491	9.80×10^{-2}	1.94×10^{15}	2.11×10^{-16}
B8	575	1.183	1.99×10^{16}	(r)1.48×10^{-14}(p)
				(v)2.35×10^{-14}(g)
B9	601.2	2.361	3.89×10^{16}	(r)6.15×10^{-14}(p)
				(v)6.79×10^{-14}(m)
			Av.	6.47×10^{-14}
	Tube length = 0.2 cm.			
34	563	0.983	1.69×10^{16}	(r)2.02×10^{-16}(m)
				(v)2.25×10^{-16}(m)
			Av.	2.14×10^{-16}
35	600	2.32	3.75×10^{16}	1.50×10^{-15}
36	621	3.84	5.67×10^{16}	4.0×10^{-15}
37	651	7.57	1.14×10^{17}	(v)10.5×10^{-15}
38	699	19.86	2.75×10^{17}	(v)2.31×10^{-14}(m)
52	660	9.18	1.34×10^{17}	2.02×10^{-14}
	Tube length = 0.196 cm.			
62	664	9.98	1.45×10^{17}	(v)1.1×10^{-14}
63	721	29.58	3.97×10^{17}	(v)2.54×10^{-14}(g)
64	766	62.23	7.87×10^{17}	(v)7.18×10^{-14}(g)

I

C_2	C_1/C_2	$\frac{C_1}{N^2 f_1^2 z_x}$	$\frac{C_2}{N^2 f_2^2 z_x}$
1.13×10^{-19}	2.50	2.16×10^{-47}	3.46×10^{-47}
1.50×10^{-18}	3.17	1.19×10^{-47}	1.52×10^{-47}
1.06×10^{-18}	3.09	1.19×10^{-47}	1.53×10^{-47}
5.7×10^{-17}	3.70	1.68×10^{-47}	1.82×10^{-47}
6.51×10^{-15}	3.61	1.78×10^{-47}(g)	1.97×10^{-47}
1.96×10^{-14}			
1.65×10^{-14}			
1.80×10^{-4}	3.60	1.31×10^{-47}	1.42×10^{-47}
0.667×10^{-16}			
0.594×10^{-16}			
0.630×10^{-16}	3.40	0.843×10^{-47}	$.947\times10^{-47}$
4.69×10^{-16}	3.21	1.20×10^{-47}	1.50×10^{-47}
1.32×10^{-15}	3.0	1.40×10^{-47}	1.84×10^{-47}
(r)3.7×10^{-15}	2.8	0.892×10^{-47}	1.28×10^{-47}
(r)0.76×10^{-14}(p)	3.04	0.344×10^{-47}	$.452\times10^{-47}$
0.597×10^{-14}	3.37	1.27×10^{-47}	1.49×10^{-47}
(r)4.13×10^{-15}	2.66	0.600×10^{-47}	0.902×10^{-47}
(r)0.95×10^{-14}(p)	2.67	0.185×10^{-47}	0.276×10^{-47}
(r)3.10×10^{-14}(p)	2.32	0.133×10^{-47}	$.229\times10^{-47}$

From (7)

$$C = \frac{\rho\gamma}{2\pi}\log_{10}e = \frac{\pi e^2\lambda_o^2}{mc^2}\frac{Nf\,x\,\gamma}{2\pi}\log_{10}e \quad (16)$$

If the above three γ's were used:

From (13)

$$C = \left(\frac{e^2\lambda_o^4\rho^2\overline{v}}{2mc^3}\log_{10}e\right) N^2 fx\ (cm^2) \quad (17)$$

From (14)

$$C = \left(\frac{e^4\lambda_o^5\cdot\log_{10}e}{4\pi m^2c^4}\right) N^2f^2x\ (cm^2) \quad (18)$$

From (15)

$$C = \left(\frac{e^4\lambda_o^5\log_{10}e}{12\ m^2c^4}\right) N^2f^2x\ (cm^2) \quad (19)$$

So the ratio of C for the two components of the lines will be: from (17)

$$\frac{C_1}{C_2} = \left(\frac{\lambda_1}{\lambda_2}\right)^4 \frac{f_1}{f_2} = 1.86 \quad (20)$$

and from (18) or (19)

$$\frac{C_1}{C_2} = \left(\frac{\lambda_1}{\lambda_2}\right)^5 \left(\frac{f_1}{f_2}\right)^2 = 3.64 \quad (21)$$

when the conventional f-value $f_1 = \frac{2}{3}$ $f_2 = \frac{1}{3}$

($\lambda_1 = 7947.64$, $\lambda_2 = 7800.29$) were used.

In Table I are listed the experimental values of C_1/C_2. The mean values of the ratio are 3.2 for pressures below 1 mm. Hg. and 3.1 for all pressures observed.

TABLE II

Plate No.	N	$(\Delta\nu_{\frac{1}{2}})_s$	$(\Delta\nu_{\frac{1}{2}})_l$	$(\Delta\nu_{\frac{1}{2}})_s/N$ x10^{-7}	$(\Delta\nu_{\frac{1}{2}})_l/N$ x10^{-7}	$(\Delta\nu_{\frac{1}{2}})_s/(\Delta\nu_{\frac{1}{2}})_l$
A2	4.42×10^{13}	8.12×10^{6}	6.25×10^{6}	1.84	1.41	1.30
A3	2.44×10^{14}	2.58×10^{7}	1.51×10^{7}	1.06	0.62	1.70
B2	2.88×10^{14}	3.02×10^{7}	1.81×10^{7}	1.04	0.63	1.67
B4	1.94×10^{15}	2.78×10^{8}	1.50×10^{8}	1.43	0.77	1.85
34	1.69×10^{16}	1.22×10^{9}	7.15×10^{8}	0.72	0.42	1.70
B8	1.99×10^{16}	3.02×10^{9}	1.67×10^{9}	1.51	0.84	1.80
B9	3.89×10^{16}	4.25×10^{9}	2.37×10^{9}	1.09	0.60	1.80
35	3.75×10^{16}	3.99×10^{9}	2.31×10^{9}	1.06	0.61	1.72
36	5.67×10^{16}	6.74×10^{9}	4.46×10^{9}	1.19	0.79	1.50
37	1.14×10^{17}	8.64×10^{9}	6.21×10^{9}	0.76	0.54	1.40
52	1.34×10^{17}	1.44×10^{10}	8.53×10^{9}	1.80	0.63	1.68
62	1.45×10^{17}	7.52×10^{9}	5.25×10^{9}	0.52	0.36	1.43
38	2.75×10^{17}	8.08×10^{9}	5.33×10^{9}	0.29	0.19	1.51
63	3.97×10^{17}	6.27×10^{9}	4.68×10^{9}	0.16	0.12	1.34
64	7.87×10^{17}	8.93×10^{9}	7.69×10^{9}	0.11	0.09	1.16

TABLE III

Plate No.	$\log_{10} N$	$\log_{10}(\Delta\nu_{\frac{1}{2}})_s$	$\log_{10}(\Delta\nu_{\frac{1}{2}})_l$
A2	13.6454	6.9096	6.7959
A3	14.3874	7.4116	7.1790
B2	14.4594	7.4800	7.2577
B4	15.2878	8.4440	8.1761
34	16.2279	9.0864	8.8543
B8	16.2989	9.4800	9.2227
B9	16.5899	9.6284	9.3747
35	16.5740	9.6010	9.3636
36	16.7536	9.8287	9.6493
37	17.0569	9.9365	9.7931
52	17.1271	10.1584	9.9309
62	17.1614	9.8762	9.7202
38	17.4393	9.9069	9.7267
63	17.5988	9.7973	9.6702
64	17.8960	9.7509	9.8859

The last four points have very poor accuracy greatly due to the error in getting the value of N by far extrapolation of formula (11). They are generally too low in the graph and are not plotted in Fig. 6.

This result appears to be in favor of the theory of (21); whereas Hughes and Lloyd's result for K resonance lines was in harmony with the corresponding theory for (20).

Further check of the equations (18) and (19) was made by calculating the values

$$\frac{C_1}{N^2 f_1^2 x} \quad \text{and} \quad \frac{C_2}{N^2 f_2^2 x}$$ which are listed in

the last two columns of Table I. These values turn out to be quite close in agreement with the theory.

(b) Relation between ~~half~~ at half maximum width and N

The relation between the half width and N is shown in Tables II and III. Results indicate that the broadening of the shorter wavelength component is greater than that of the longer wavelength component by a factor of 1.6. For low pressures

$$(\Delta\nu_{\frac{1}{2}})_s = 1.2 \times 10^{-7} N \quad \text{sec}^{-1} \qquad (22)$$

$$(\Delta\nu_{\frac{1}{2}})_\ell = .77 \times 10^{-7} N \quad \text{sec}^{-1} \qquad (23)$$

These values will be still smaller if the data for higher vapor pressures were considered. The difference of the broadening of the two doublet components is not what expected from Prof. Houston's theory but so far the relation of the half widths and the concentration N is concerned, this result is in much closer agreement with his theory than is

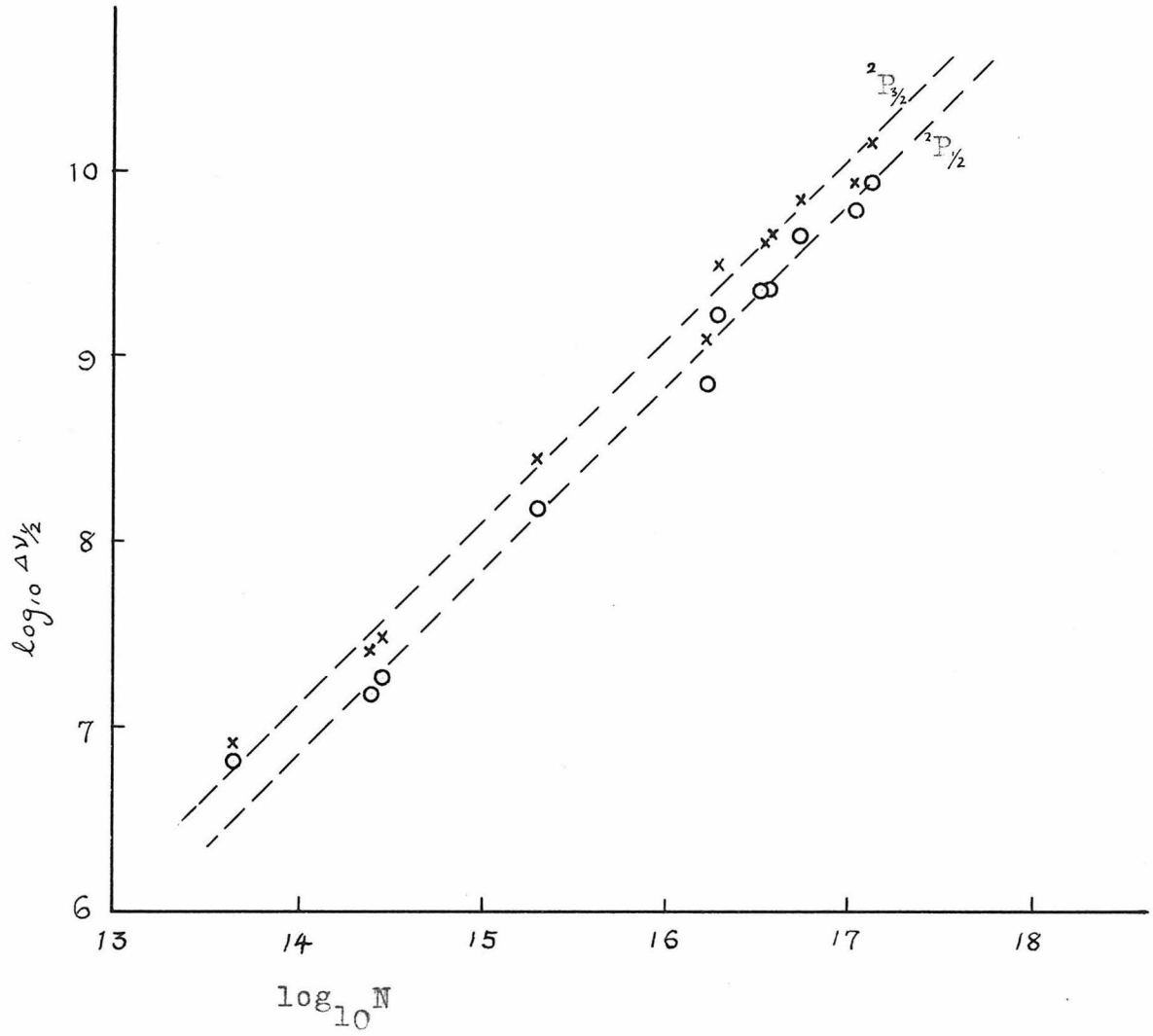

Fig. 6 The relation between $\Delta\nu_{1/2}$ and N

the corresponding one obtained by Drs. Hughes and Lloyd. Lloyd's value showed a factor of ~~10~~ 5 too high while in the present research the values for low pressures are only ~~3.8~~ 1.9 and ~~2.4~~ 1.2 times higher for the two components respectively. If the values for all pressures were taken into consideration.

$$(\Delta\nu_{\frac{1}{2}})_s = .96 \times 10^{-7} N \qquad (24)$$

$$(\Delta\nu_{\frac{1}{2}})_1 = .55 \times 10^{-7} N \qquad (25)$$

These were only 3 and 1.7 times higher (for the two components respectively) than Prof. Houston's theoretical value.

In Fig. 6 are plotted the values of $\log_{10} N$ against $\log_{10}(\omega\nu_{\frac{1}{2}})$ as given in Table III. A straight line of unit slope can be drawn through those points, showing the proportionality of the width with N.

B. Observation of the Line Broadening under Higher Pressures

(a) The asymmetrical line contour

As mentioned before, when the temperature of the tube was raised to about 290°C or more (or for pressures higher than 1 mm. Hg.) the lines showed more and more asymmetrical broadening. The $^2P_{\frac{1}{2}}$ component shows asymmetry towards the red; while the $^2P_{3/2}$ component towards the violet. Fig. 8 is the coefficient of absorption curve showing this circumstance. Naturally the dispersion formula will no longer be valid. Consequently the former method of evaluating C will not be justified as no

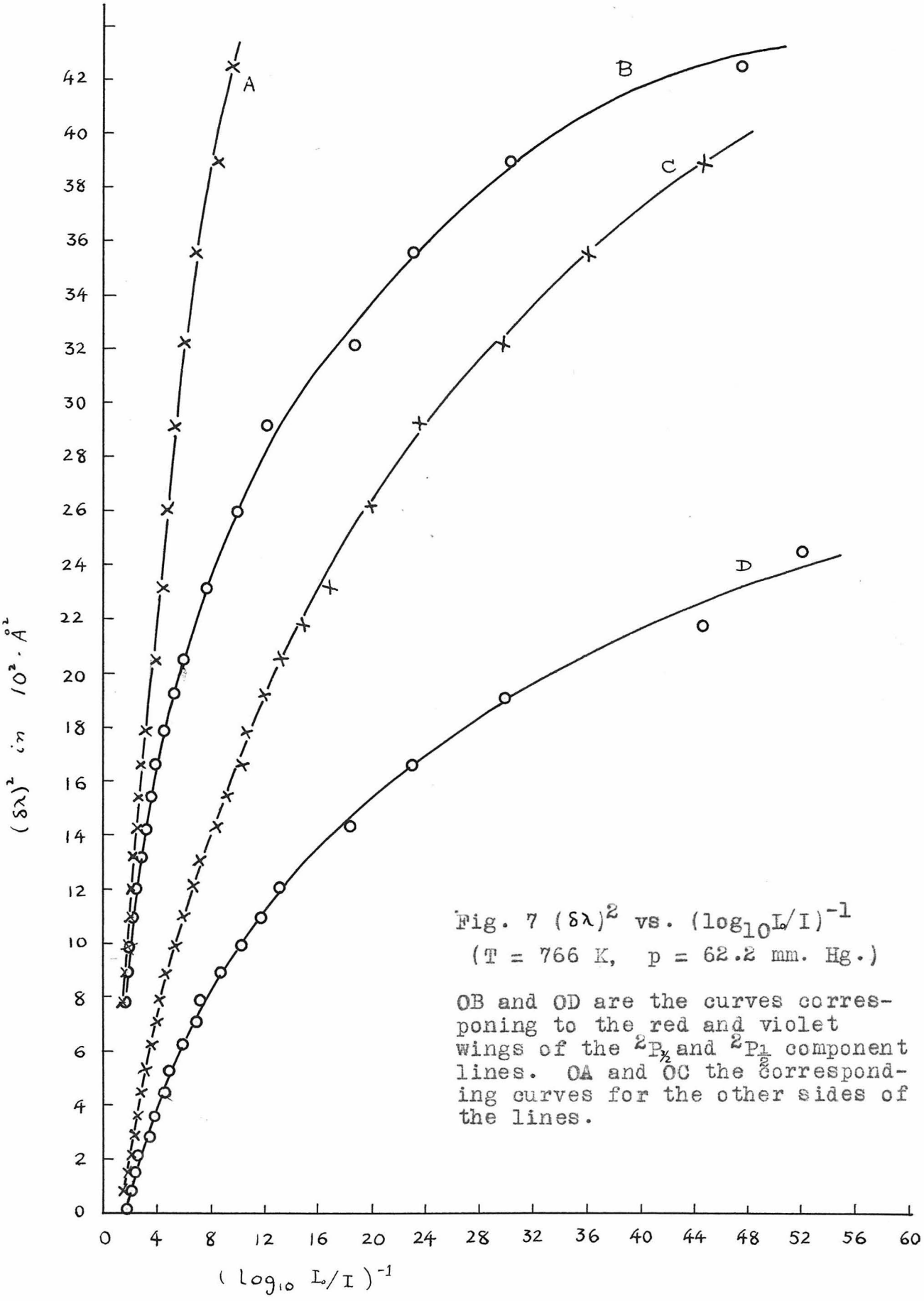

Fig. 7 $(\delta\lambda)^2$ vs. $(\log_{10} L_0/I)^{-1}$
(T = 766 K, p = 62.2 mm. Hg.)

OB and OD are the curves corresponing to the red and violet wings of the $^2P_{\frac{3}{2}}$ and $^2P_{\frac{1}{2}}$ component lines. OA and OC the corresponding curves for the other sides of the lines.

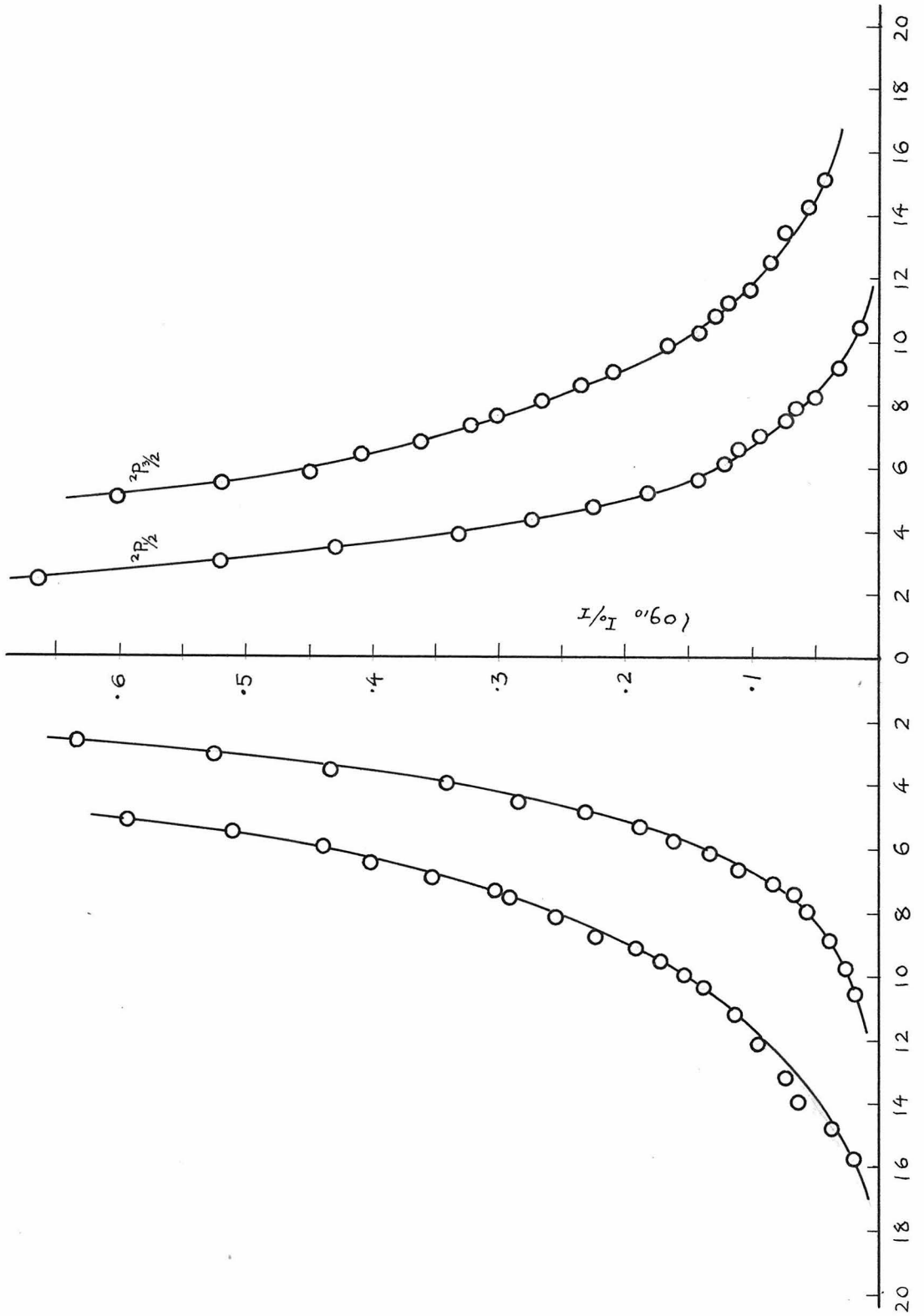

Fig. 8a. The asymmetrically broadened lines for Plate No. 35
(T = 600°K p = 2.32 m.m. x = 0.2 cm.)

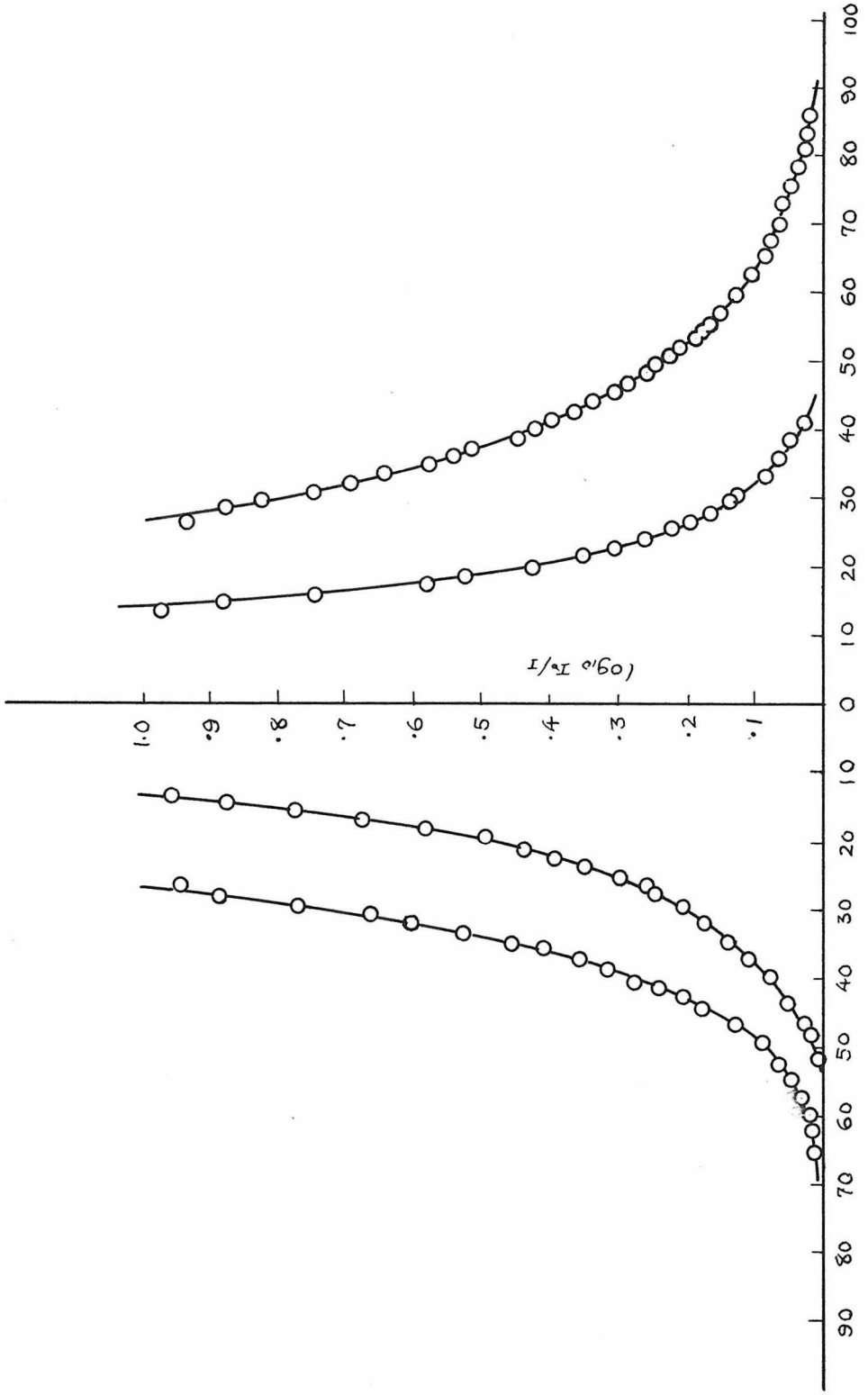

Fig. 8b The asymmetrically broadened lines for Plate No. B9

(T = 601°K p = 2.36 m.m. x = 7.50 cms.)

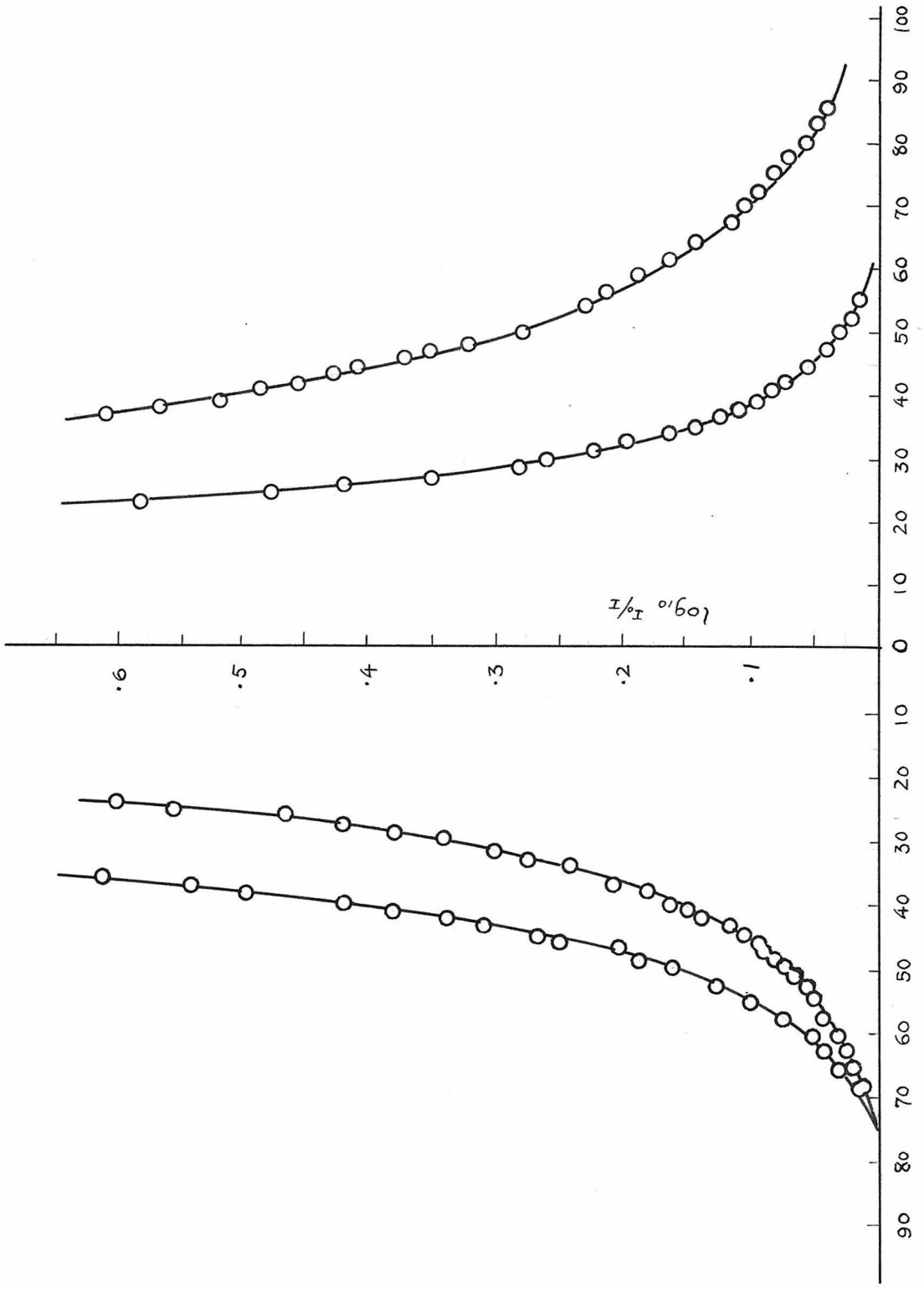

Fig. 8c The asymmetrically broadened lines for Plate No. 64
(T = 766°K p = 62.2 mm. x = 0.196 cm.)

good straight line could be drawn in the $(d\lambda)^2$ vs. $(\log \frac{I_o}{I})^{-1}$ plot, as before. A typical result is shown in Fig. 7.

A test of the applicability of the dispersion formula used before was also made on these asymmetrical lines. Results showed that in general a fairly straight line for C (as shown in Fig. 7) could be drawn for the shorter wavelength side of the $^2P_{3/2}$ component and for the longer wavelength side of the $^2P_{\frac{1}{2}}$ component. These values are also listed in Table I. The letters (r) or (v) written before the numerical values of C indicate that the values were evaluated according to the red or the violet wing of the lines. The letters (p), (m), (g) after the numerical values show the quality of the curve in evaluating C: (p) means poor designating that the experimental points did not yield a nice straight curve in obtaining the slope C; (m) means medium; and (g) means good showing that the experimental points yield a very good straight line for the determination of C.

Unfortunately no dispersion formula was found which will discribe completely these asymmetrically broadened lines. So the contours of the lines were presented in Figs. 8 for Plate Nos. B9, 35, and 64. Note the asymmetries of the component lines.

The fact that the shorter wavelength side of the $^2P_{\frac{1}{2}}$ component and the longer wavelength side of the $^2P_{3/2}$ component do not follow the dispersion formula (3) is not only due to the asymmetry; a faint band was observed near each of the component

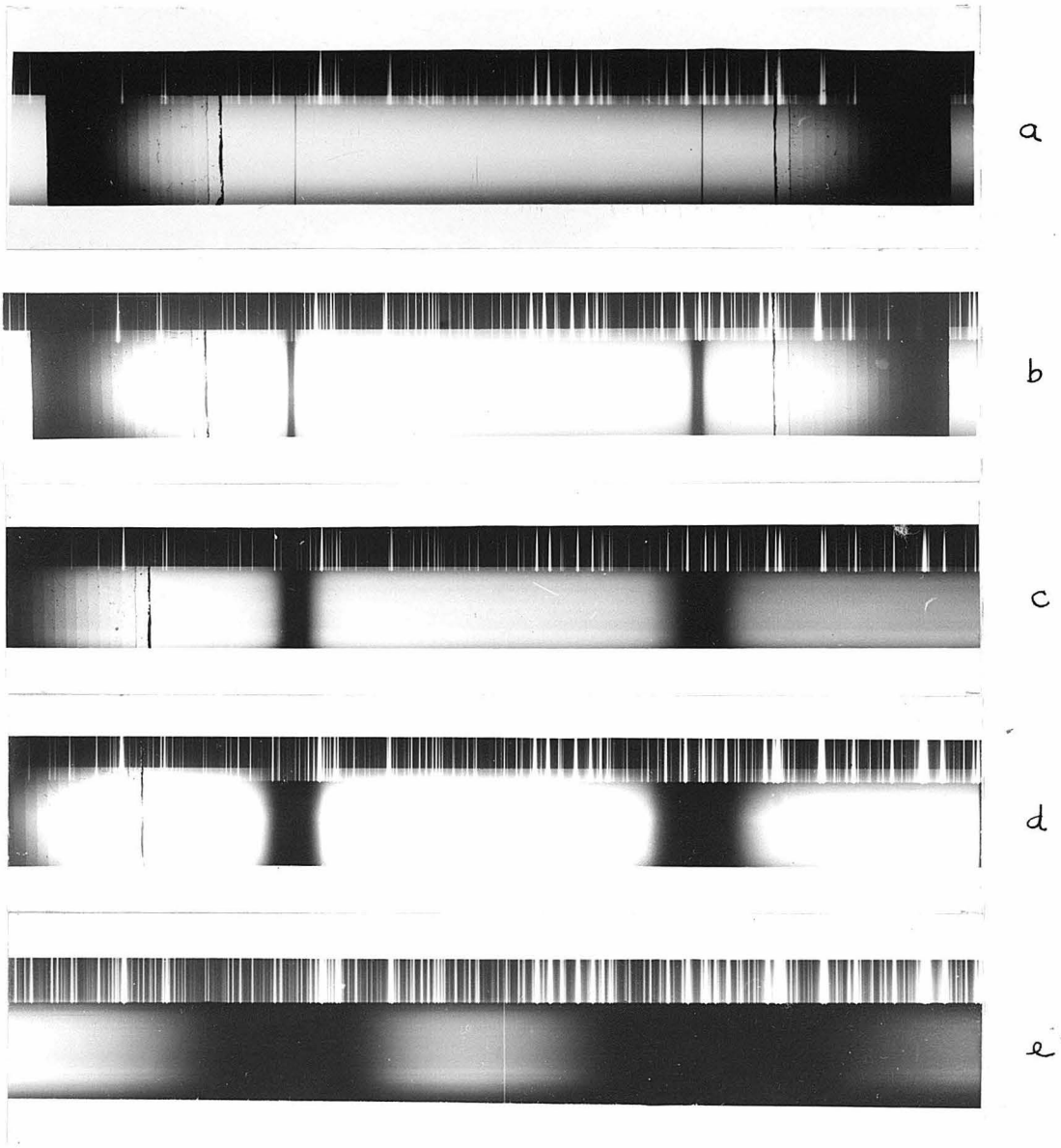

Fig. 9 Photograms showing the broadening of the lines at different temperatures

(a) Plate 22 T=180 C (b) Plate 34 T=290 C
(c) Plate 36 T=348 C (d) Plate 37 T=378 C
(e) Plate 65 T=524 C

lines at these very sides of the lines. This phenomenon will be discussed in detail under a separate paragraph.

(b) The extension of the width of the line with pressure and tube length

The broadening of the lines can be described qualitatively by reviewing carefully the 39 plates both analysed and unanalysed. The spectrograms reproduced in Fig. 9 are quite illustrative. The lines were quite symmetrically broadened when the pressure was below about 1 mm. when the pressure was raised the lines tend to broaden unsymmetrically; and at about the same time the faint band in the neighbourhood of the doublet components become strong enough to be perceptible in the spectrogram (see Figs. 10 and 11), one on the red side of $^2P_{3/2}$ and one on the violet side of $^2P_{\frac{1}{2}}$. When the pressure was again raised the asymmetry and the increase in intensity of those faint bands brought the line and the band together causing a faint shadow (see Fig. 9c). Then when the pressure was again increased the intensity of the band became much larger than the wing of the line so a clear cut edge of density is shown in the plate (see Fig. 9d). The edge should be still sharper if the intensity of the background was uniform all over the width of the spectrum.

Thus it is evident that it is the doublet lines whose broadening is considerably increased with the increase of N, the concentration; the band is not appreciably broadened.(17)

---

(17) The intensity of the band is increased, because when the concentration of Rb vapor is increased, the probability of producing the band will be naturally raised.

The additional absorption due to the band results an increase in the steepness at that side of the line contour. Finally when the pressure was further raised the resonance broadening of the component lines become so large that the band was completely masked, so only a strong asymmetry could be observed (Fig. 9e).

It is interesting to note that the line contours for plates No. B9 and No. 35 correspond to nearly the same concentration N ($601^{\circ}K$) but with different tube lengths (7.50 cm and 0.2 cm, a factor of 38). For the longer tube length one (Plate No. B9) the absorption is comparatively much larger than that of the shorter one. So in determining the line contour measurements were made at large $d\nu$'s which will show more asymmetry according to the van der Waals distribution. While for the shorter tube length one (Plate No. 35) the absorption was much smaller, so measurement could be made at smaller $d\nu$'s. So Plate No. 35 showed much symmetrical contours.

(c) Test of Kuhn's $-3/2$ law

At these high pressure, the line was considerably broadened. Thus measurements of the line contours were actually made at the wings of the line corresponding to large frequency changes. So Kuhn's $\Delta\nu^{-3/2}$ law[18] of intensity was tested by letting

---

(18) Kuhn's $\Delta\nu^{-3/2}$ law.

$$\alpha x = (2\pi ANC^{\frac{1}{2}}/3)/(\nu_0 - \nu)^{3/2}$$

where $A = (\frac{\pi e^2}{mc})Nfx$

N = no. of atoms per c.c.
x = length of the absorbing column
C is a constant of the transition.

$$\alpha x = \text{const } (N^2 fx)\ (\nu_0 - \nu)^{-a} \tag{26}$$

or $$2.3 \log_{10} \frac{I_0}{I} = \text{const } N^2 fx\ (\nu_0 - \nu)^{-a} \tag{27}$$

$$\log_{10}\left[\frac{2.3}{\text{const } N^2 fx} \log_{10} \frac{I_0}{I}\right] = -a \log_{10}(\nu_0 - \nu)$$

$$= -a \log_{10} d\nu = -a \log_{10}\left(\frac{-c}{\lambda^2} d\lambda\right)$$

$$= -a \log_{10} d\lambda - a \log_{10}\frac{c}{\lambda^2}$$

$$= -a \log_{10} d\lambda + K_1 \tag{28}$$

For certain particular temperature of the absorbing column of certain length, and certain line, Nfx are constants. Hence the formula reduces to

$$\log_{10}(\log_{10} \frac{I_0}{I}) = -a \log_{10} d\lambda + K_2 \tag{29}$$

or $$\log_{10} D = -a \log_{10} d\lambda + K_3 \tag{30}$$

The value of "a" as obtained by finding the slope of the plot of $\log_{10} D$ vs. $\log_{10} \delta\lambda$ is considerably greater than $-3/2$. Table IV gives some values of "a" as obtained from different spectrograms.

Table IV

Plate No.	N	x cm	a for $^2P_{\frac{1}{2}}$	$^2P_{3/2}$
B9	3.89×10^{16}	7.50	(r)2.00 (v)2.85	(r)3.12 (v)2.50
64	7.87×10^{17}	.2	(r)2.85 (v)3.47	(r)3.92 (v)2.53

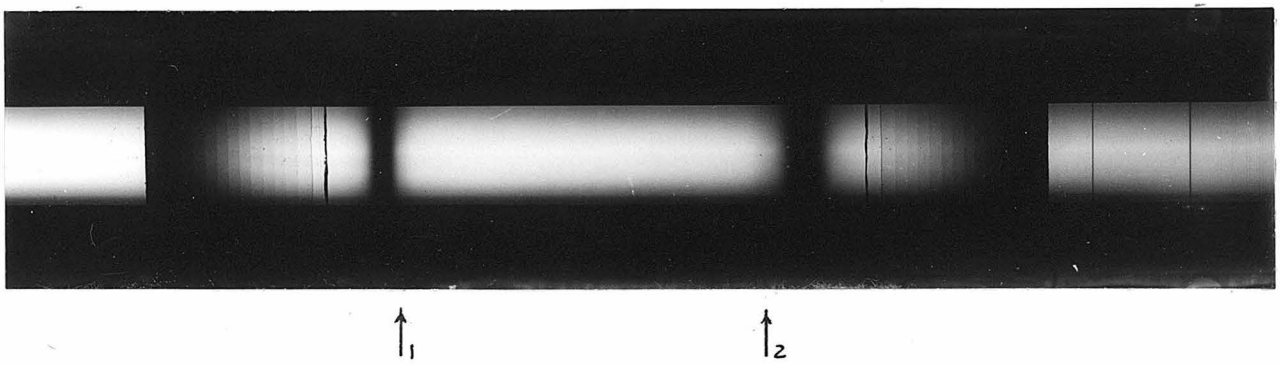

Fig. 10 The new absorption bands
(Plate No. B7, T=257 C)

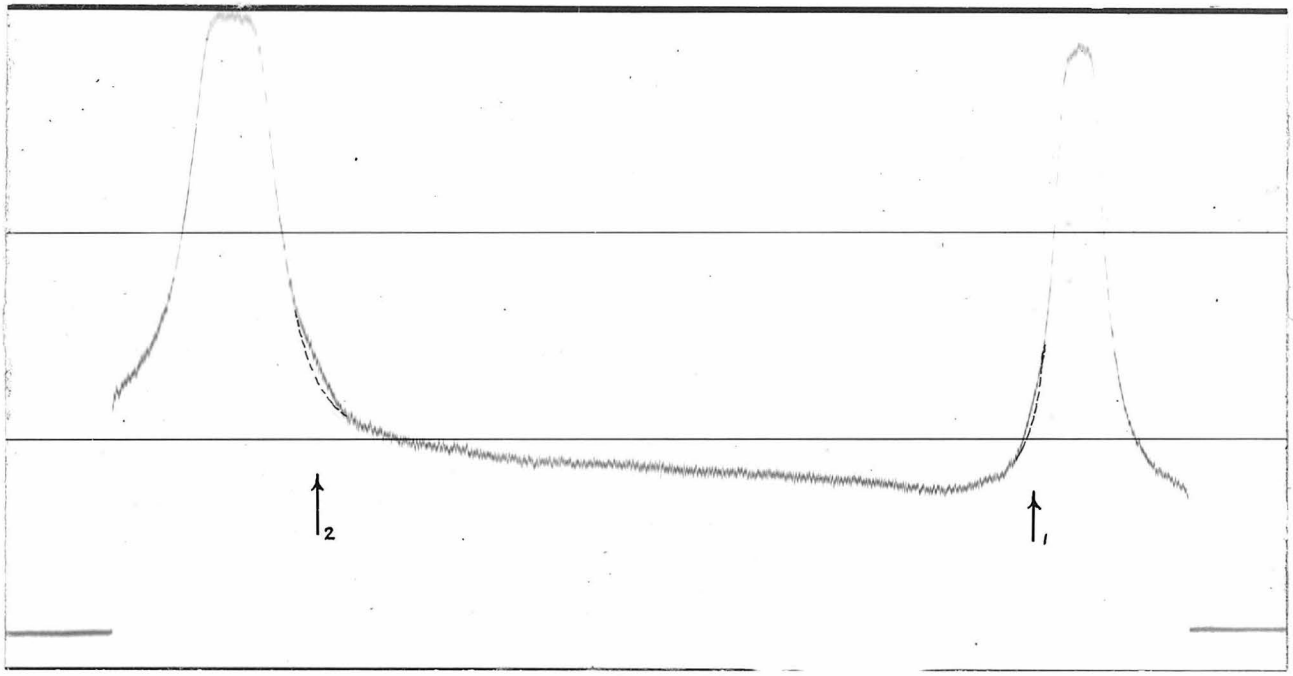

Fig. 11 The microphotometer curve
of Plate No. B7

The above result is hardly a comfirmation of Kuhn's formula. This is also the case for K resonance lines as pointed out by Hughes and Lloyd(4).

(d) The Band

The band appearing near the shorter wavelength side of the $^2P_{\frac{1}{2}}$ component and near the longer wavelength side of the $^2P_{3/2}$ component calls for considerable attention. Note Fig. 9c, Fig. 10, and Fig. 11. Owing to the fact that the bands are located quite near to the doublet lines the position of these bands could not be determined with good accuracy, but the violet side edge of the band near the $^2P_{\frac{1}{2}}$ component and the red side edge of the band near the $^2P_{3/2}$ component could be easily located. The data were:

	Band a	Band b
The position of band	7967.5 Å ;	7812.7 Å
The approximate width of the band	5.7 Å ;	10.2 Å

The biolet edge of band a at 7964.5 Å

The red edge of band b at 7817.6 Å

In order to obtain these bands it is advisable to use a long absorption tube and to adjust the time of exposure (not the time of development), so that the density of the spectrum is not too high. In the present experiment the bands appeared most clearly in Plate B9, 36, 52 and 62. The experimental conditions for the respective spectrograms were tabulated as the following:

Plate No.	T	p mm.Hg	N	Tube length
B7	530° K	0.306	5.61×10^{15}	7.50 cms.
36	621	3.84	5.67×10^{16}	0.2 cm.
52	660	9.18	1.34×10^{17}	0.2 cm.
62	664	9.98	1.45×10^{17}	0.196 cm.

The presence of these bands was previously unknown. These bands might be due to loosely bound molecules formed by polarization forces during the time of collisions. A band interpreted as due to polarization molecules has been observed by Kuhn[19] at the violet side of the second doublet of Cs principal series and some bands for K_2, Na_2. Ny and the author[20] have observed the corresponding band in the neighbourhood of Rb second doublet of the principal series. These bands may be the corresponding polarization bands in the neighbourhood of the resonance lines. Nevertheless, the positions of the bands here observed (one on the shorter wavelength side and the other on the longer wavelength side of the doublet lines) were irregular. As suggested by Prof. Houston this phenomenon might be due to the coupling between the two doublet components. In Hughes and Lloyd's paper the asymmetries of lines were observed only when the pressure was raised to 20 mm. Hg, and no band was seen in the neighbourhood of K lines. If they have not overlooked the

---

(19) H. Kuhn, Zeit. f. Physik, 76, 782, 1932.

(20) Ny Tsi-ze and Ch'en Shang-yi, Nature 138, 1055, 1936; J. de Physique, T. 9, S.7, 169, 1938.

the phenomena, one might draw the conclusion that it might be more pronounced for those doublet lines whose fine structure intervals are large.

(e) The reversal of the lines

Another interesting phenomenon observed was that shown in Fig. 9b. The central parts of the strongly absorbed lines showed instead of complete clearness on the plate a dark strip at the position corresponding to the central maximu. In Plate Nos. 34 and 61 (temperatures were 563°K and 613°K respectively) the phenomenon was most clear.

This phenomenon can be explained according to the idea of self reversal in emission lines. The frequencies of the radiation from the incandescent lamp corresponding to those of the Rb resonance lines were all absorbed when they were passing through the absorption tube by Rb atoms. The valence electron of Rb was excited during the process of absorption. Accordingly the excited electron has to return to its normal state, $^2S_{\frac{1}{2}}$, by the emission of the same frequency. But all light from the incandescent lamp passed through the absorption tube was used to fill the slit of the spectrograph, while the light emitted by the atoms radiated in all directions; the part that could go into the slit of the spectrograph was very small in comparison with the background light. So only in favorable conditions the frequency corresponding to the central maximum of the line showed the emitted energy.

(f) The Rb_2 band

Rubidium band spectra observed from far infra red up to about 7800 Å. These bands have been studied by Matuyama[21] and others and are classified as due to the transitions of $^1\Pi$ -- $^1\Sigma$ and $^1\Pi$ -- $^2\Sigma$ for the red and infra-red regions.

(g) The shift

The displacement of the absorption maxima of the lines could not be determined with good certainty. The lines corresponding to high vapor pressures would show more shift, but due to their great increase in width and asymmetry, their positions of maxima could hardly be located. The following are the results of measurement:

Plate No.	T °K	p mm.Hg	Shift in Å $^2P_{\frac{1}{2}}$	$^2P_{3/2}$
62	664	9.98	.05(r)	.96(v)
63	721	29.6	.74(r)	1.32(v)
64	766	62.2	2.8 (r)	4.99(v)

Although too much emphasis can not be put on the accuracy of the measurement, yet it is safe to say that the $^2P_{\frac{1}{2}}$ component shows a shift towards the red while the $^2P_{3/2}$ component shows a violet shift. This follows the general statement (so far

---

(21) Matuyama, Tohoku Imp. Univ. Sci. Rep. 23, 308, 1934.

with only one exception[22]) about the relation between the shift and the asymmetry for pressure effects on spectral lines by foreign atoms that the shift of the maximum of absorption is accompanied by a asymmetry towards the same direction.

---

(22) For Cs 3876 perturbed by N_2, a red shift of the maximum of absorption is accompanied by a violet asymmetry, C. Füchtbauer and F. Gössler, Z. f. Physik, 93, 648, 1935.

VI CONCLUSION

The widths of the broadened resonance lines of Rb agree with Margenau and Watson's derivation. Under pressures below 1 mm. the lines are very symmetrical. The broadening of the shorter wavelength component is greater than that of the longer wavelength component. The half widths of both components are proportional to the density and are greater than that predicted by Prof. Houston's theory by a factor of ~~3.~~ 1.5

The lines exhibit asymmetrical broadening when the pressure is above 1 mm. Hg. The $^2P_{\frac{1}{2}}$ component shows red, while the $^2P_{3/2}$ component shows violet asymmetry. The fact that the shorter wavelength side of the $^2P_{\frac{1}{2}}$ component and the longer wavelength side of the $^2P_{3/2}$ component deviate very strongly from the dispersion formula is not only due to the asymmetry but also due to the faint band appeared at the respective sides of the lines near each component of the doublet.

At the wings of the lines corresponding to large frequency changes, the intensity distribution does not follow Kuhn's $-3/2$ law. The shifts of the lines could only be roughly estimated; results showed a violet shift of the violet asymmetrical $^2P_{3/2}$ component and a red shift of the red asymmetrical $^2P_{\frac{1}{2}}$ component.

VII. ACKNOWLEDGEMENT

The author wishes to express his hearty thanks to Prof. I. S. Bowen for his kind supervision and encouragement throughout the research, and to Prof. W. V. Houston for his invaluable guidance and interest in the work. The author is also greatly indebted to Dr. P. E. Lloyd for his generosity in discussing his experiences during his research in K resonance lines.

He finally wishes to express his deep appreciation, as a foreign student, of the friendly and stimulating atmosphere at Caltech.

THESIS II

THE BROADENING, ASYMMETRY AND SHIFT OF RUBIDIUM RESONANCE LINES UNDER HOMOGENEOUS PRESSURES OF HELIUM AND ARGON UP TO 100 ATMOSPHERES

ABSTRACT

The broadening, asymmetry and shift of rubidium resonance lines produced under different pressures of pure helium and argon up to 100 atmopheres were studied. The broadening is linearly proportional to the relative densities of these gases, and is different for different doublet components. The slopes of these half-width vs. relative density curves are .735 cm^{-1} and .594 cm^{-1} per unit relative density of helium for $^2P_{1\frac{1}{2}}$ and $^2P_{\frac{1}{2}}$ components respectively, and the corresponding values for argon are .855 cm^{-1} and .627 cm^{-1} per unit relative density. Helium produces a violet, while argon a red asymmetry. The degree of asymmetry increases as the concentration of foreign gas increases, and is comparatively much greater for argon. For argon the asymmetry of the $^2P_{1\frac{1}{2}}$ component is greater than that of the $^2P_{\frac{1}{2}}$ component, while for helium the reverse is true. Argon produces a greater shift than helium. The former produces a strong red, while the latter a violet shift. For both gases the shift of the $^2P_{\frac{1}{2}}$ component is greater than that of the $^2P_{1\frac{1}{2}}$ component. For helium the shift appears to be proportional to the relative density, and the shift of the $^2P_{\frac{1}{2}}$ component is about twice as great as that for the shorter wave-length component; while for argon the shifts for the doublet components are quite close, and the relation between shifts and relative densities obeys in general the 3/2 power relationship. Optical collision diameters as calculated from the half-width data are 13.37$\mathring{A}$ and 7.753 $\mathring{A}$ for Rb-A and Rb-He respectively. From the measurement of the amount of total absorption of the line contours, f-values and the transition probabilities were evaluated. The f-values turn out to be .33 and .66 for the $^2P_{\frac{1}{2}}$ and $^2P_{1\frac{1}{2}}$ components of the Rb resonance lines respectively.

C O N T E N T S

THE BROADENING, ASYMMETRY AND SHIFT OF RUBIDIUM RESONANCE LINES UNDER HOMOGENEOUS PRESSURES OF HELIUM AND ARGON UP TO 100 ATMOSPHERES

I. INTRODUCTORY

The effects of foreign gases upon spectral lines, such as displacement, broadening and asymmetry, have opened up a new way for investigating the perturbations of the energy levels of the absorbing atom and consequently attracted the attention of many experimental and theoretical physicists. V. Weisskopf[1] H. Margenau and W. W. Watson[2], and P. Schulz[3] have given a general review on the subject with an adequate bibliography. The extent of the work on the problem can be briefly described in the form of a table, (see Table I) in which the horizontal column at the top gives the nature of foreign atoms that have been employed to perturb the absorption lines of the various alkalis given at the extreme left of the rows. The number of marks "∇" or "$\surd$" indicate the number of researches that have been done on that specific combination of absorbing and perturbing atoms. The mark "∇" indicates the research done by the writer; while the mark "$\surd$", the work done by other experimenters.

---

(1) V. Weisskopf, Physik. Zeits. 34, 1, 1933.
(2) H. Margenau and W. W. Watson, Rev. Mod. Phys. 8, 22, 1936.
(3) P. Schulz, Phys. Zeits. 39, 412, 1938.

Table I. Table of Researches on the Various Combinations of Perturbing and Absorbing Atoms.

	A	Ne	He	H_2	N_2	Xe	Kr	(ad)	(as)	(c)
Li										
Na	✓✓✓ ✓✓✓	✓ ✓ ✓	✓ ✓ ✓✓✓	✓✓✓ ✓ ▽	✓✓✓ ✓✓▽			✓	✓✓✓✓✓	✓
K	 ✓✓✓	 ✓	 ✓ ✓	✓ ✓	✓✓✓ ✓ ✓				✓	
Rb	▽ ▽ ▽	▽ ▽	▽ ▽ ▽	▽ ▽ ▽	▽ ▽			▽	▽	
Cs	✓	✓	✓	✓ ▽	✓ ▽	✓	✓		✓	✓

N. B. (ad) = alkali vapors of different kind

(as) = alkali vapors of the same kind

(C) = saturated hydrocarbons, such as methane, ethane and propene.

"▽" Researches done by the writer of this paper

"✓" Researches done by other experimenters.

After the discovery of the corrosion resistant Mg O windows [4] there is still a difficult problem confronting experimental physicists. The problem is that of the construction of a high pressure absorption chamber whose windows could continue to be pressure tight after the absorption tube had been heated and then cooled. Margenau and Watson [5] made with considerable trouble, an absorption tube, where windows could be heated; but they confessed to only partial success at overcoming the leakage. With this absorption tube they studied nitrogen in potassium up to 30 atmospheres. As yet no other high pressure observations with more improved absorption tube had been made. Up till the present high pressure absorption tubes were still made in the old form with water cooling on both ends[6]. But this has several disadvantage [7]. Otherwise the whole tube and the windows had to be made of glass, so only low pressure observations were possible [8].

---

(4) See page 1 of the first article
(5) H. Margenau and W. W. Watson, Phys. Rev. 44, 92, 1933.
(6) For example: see experiments by
Füchtbauer Schulz, and Brandt, Z.f.Physik, 90, 403, 1934.
Ny Tsi-Ze and Ch'en Shang-yi, Phys. Rev. 51, 567,1937; 54, 1045, 1938.
Füchtbauer and Heeser Z.f.Physik, 113, 323, 1939.
(7) This problem will be discussed in detail in chapter II.
(8) For instance: see Füchtbauer and Gössler, Z.f.Physik, 87, 89, 1933.

In the present research, an absorption tube was made which is perfectly pressure tight both at low and at high pressures. So the pressure effects of He, A, on the resonance lines of rubidium was studied under pressures up to 100 atmospheres (also with hydrogen up to 20 atmospheres). Furthermore, Mg O windows were used so that the length of the optical path in the rubidium vapor was known. The optical collision diameters, and the areas under the absorption line contours were determined leading to the evaluation of the oscillator strength of the atom and the transition probabilities.

II. EXPERIMENTAL

(a) The absorption tube

It is not hard at all to make a vessel which is pressure tight. Also it should not be difficult to construct a pressure tight absorption tube with two transparent windows kept at a certain constant temperature. But the problem of making an absorption tube with windows pressure tight both at low and at high temperatures has up till now been unsolved.

Margenau and Watson [5] attempted to solve the problem by holding a glass window on the ends of the absorption tube by means of overlapping nuts threaded on to the tube. Lead rings were used, their lateral expansion when compressed being hindered by short sections of thin-walled steel tubing which fitted tightly into the main tube and the end nuts. As pointed out by themselves, considerable trouble was experienced in constructing the gaskets and the leaking was not completely overcome.

In using absorption tube with cooled windows not only is it not possible to determine many physical constants from the measurement of the absolute absorption coefficients because the optical path of the absorbing vapor is unknown, and neither the absorbing nor perturbing atom have a homogeneous concentration in the tube, but also experimental troubles arise of the kind pointed out by Dr. Ny and the author [9]

---

(9) Ny Tsi-Ze and Ch'en Shang-Yi, Phys. Rev. 54, 1045, 1938.

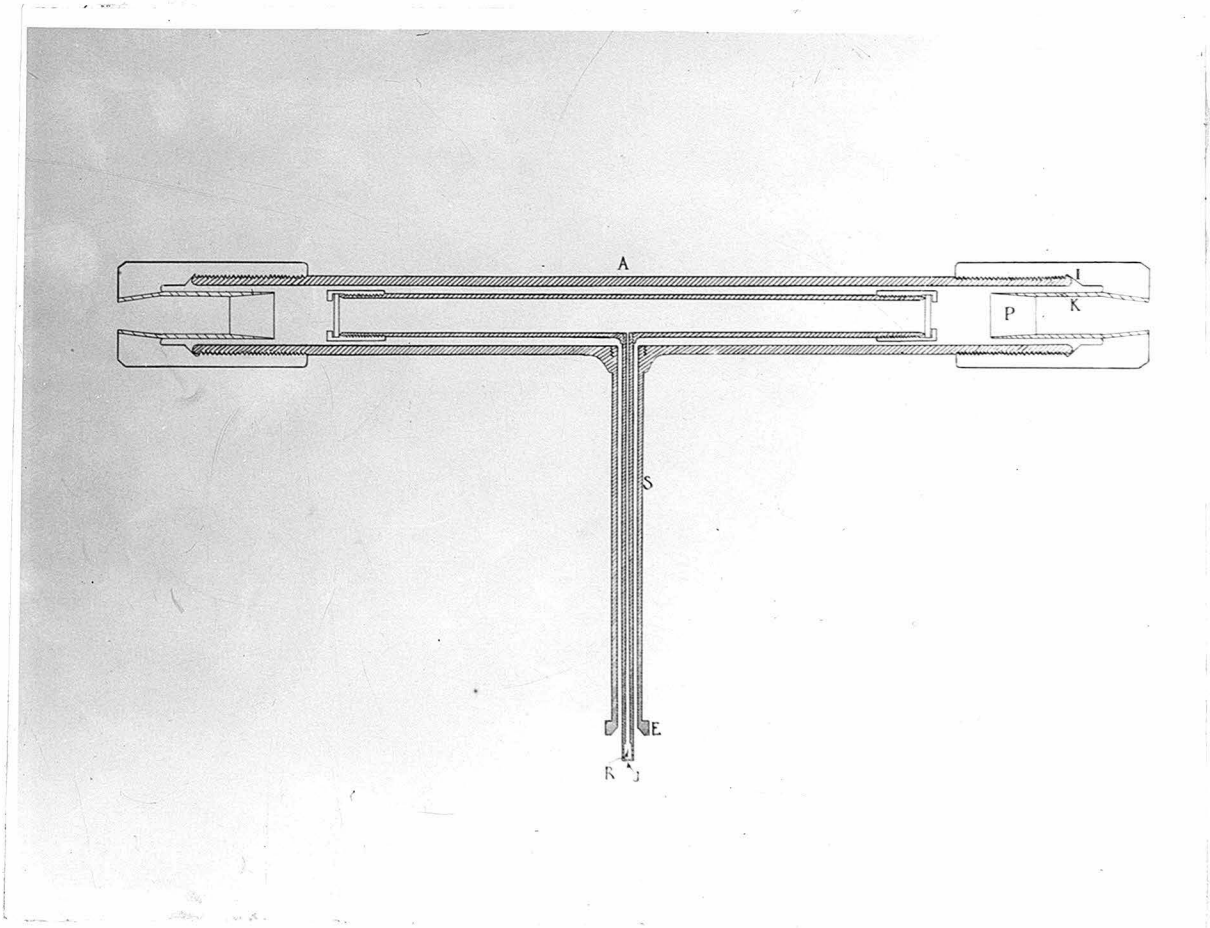

Fig. 1. The pressure tube

A-- The pressure tube
E-- Ending for the union joint
I-- Inclined plane on window frame
J-- Small hole joining the pressure tube and the inner absorption tube
K-- Kovar cone
P-- Pyrex glass window
R-- Reservoir for condensed Rb vapor
S-- Side tube

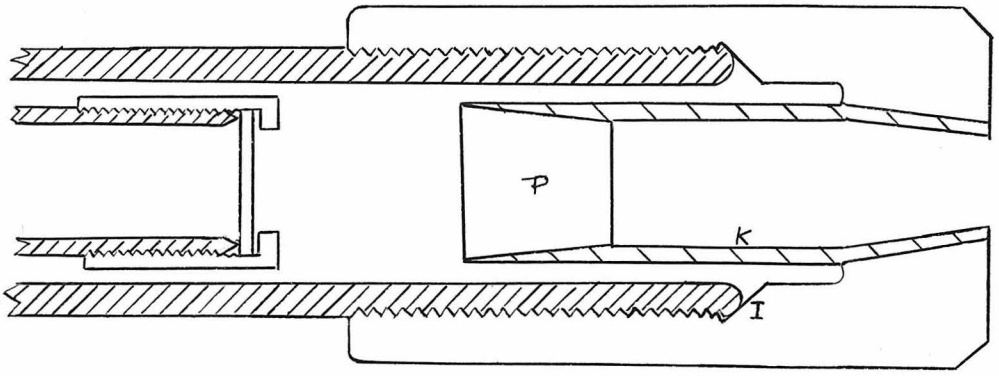

Fig. 2. The pressure window

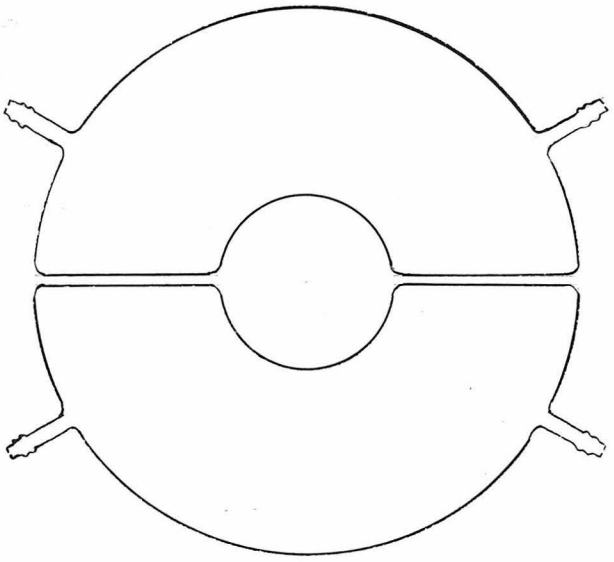

Fig. 4. The water cooler

and later confirmed by Fűchtbauer and Heesen [10].

In the present research a thoroughly satistactory high pressure absorption tube was constructed. This development will make feasible the solution of many physical problems.

The construction of the tube is shown in Fig. 1. A is a steel pressure tube 1⅛ inch in diameter with 3/16 inch wall thickness. At the middle of the tube was connected very strongly by iron soldering a side-tube S about 7 inches long whose end E was ready to connect by a union with a cross tube as shown in Fig. 2. Inside the pressure tube was placed an inner absorption tube about 26 cms. long with Mg O windows ¾ inch in diameter and 1/8 inch thick on both ends. At the central part of the tube there was a side tube thinner than S. This thinner side-tube was screwed on to the inner absorption tube and could be taken off very easily by unscrewing. So the inner absorption tube could be easily put in position by first inserting it in the pressure tube, then connecting the side tube.

The essential difficulty in constructing the pressure tube was to make the pressure tight windows whose construction is shown in Fig. 2. The whole window frame was made of the same material as that of the main pressure tube except the pyrex glass window P and the Kovar cone K holding

---

(10) C.Fűchtbauer and W. von Heesen, Z.f.Physik, 113,323,1939.

the window. So when the window frame was screwed on to the ends of the pressure tube, the inclined part,I, of the frame will be pressed very tightly on the round and smooth end of the pressure tube, This would always serve as an excellent pressure sealing because, the tube end and the window frame would contract or expand equally at various temperatures.

The thin Kovar cone was united with the steel frame by silver soldering. Before the glass window was put in position the Kovar cone was ground so that it fit very nicely with the polished conical glass. Then very thin aluminium rings were employed in the gasket (11). The pyrex glass was pressed into the Kovar cone when the whole thing was heated to about 250°C at which the aluminium ring became soft. As Kovar metal has nearly the same coefficient of expansion as that of the pyrex glass, the window was always tightly fitted in the cone at different temperatures. A slight difference between the expansions of the two material that might occur could be compensated by the elasticity of the thin cone.

The pyrex glass window was 2 cm. thick and $\frac{3}{4}$ inch in diameter; the angle of the cone was about 5°. If the angle were greater than 7° the window would leak even with the above method. Obviously, there will be no difficulty if the pyrex

---

(11) Copper rings were tried. They did not work owing to its hardness. Gold rings would be even better than aluminium because it is softer and has a still higher melting point.

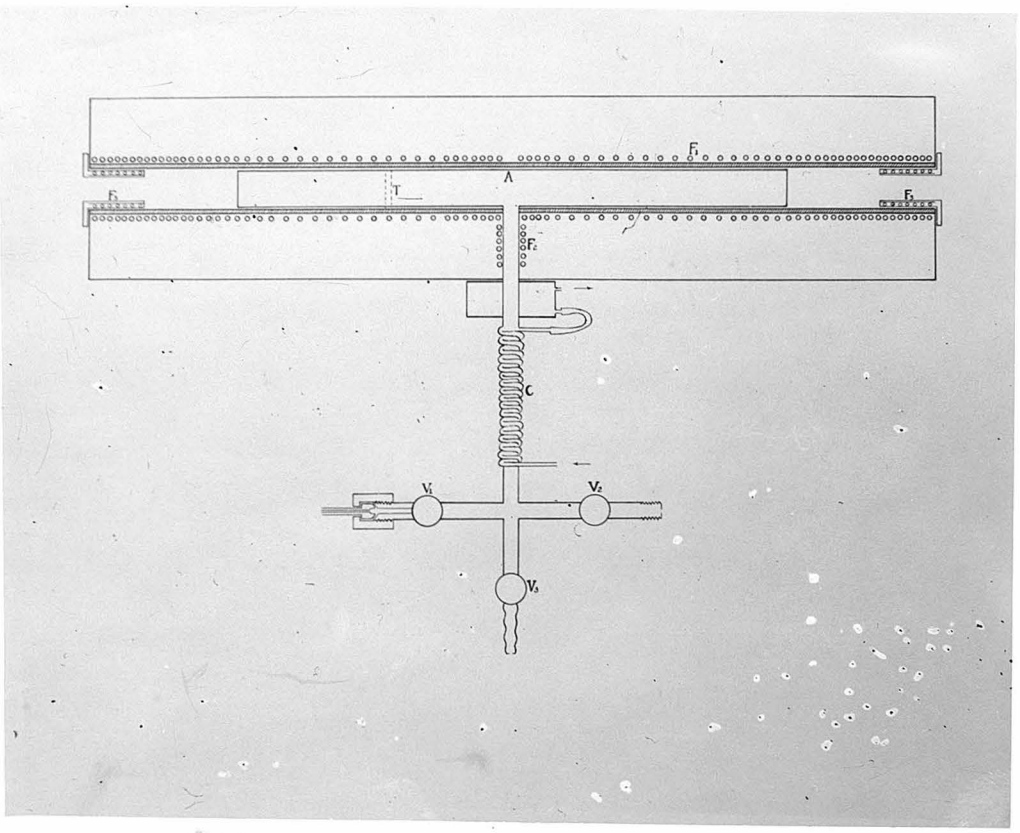

Fig. 3. The furnace

A-- The pressure tube
C-- Water coolings
F_1- The long furnace for heating the pressure tube
F_2- The furnace for heating the side tube
F_3- The heating unit for guarding the excess of heat loss from the end of the furnace when the temperature of the tube was heated above 250 C
T-- The place where the hot junction of the Alumel-Chromel thermocouple was fastened by a steel ribbon
V_1- The needle valve for inleting foreign gas
V_2- The needle valve led to the pressure gage
V_3- The needle valve connected to the vacuum pump

glass is replaced by fused quartz when observations are to be made in the ultraviolet region.

(b) The furnace.

The construction of the furnace is shown in Fig. 3. The absorption tube A, which is only schematically shown was heated by the furnace F_1. The furnace was made by winding chromel wires on steel cylinders covered by asbestos paper. The whole furnace, F_1, consisted of two sections which were connected at the position of the side tube. The windings were so made that when the side tube was heated by a small furnace, F_2, the mean absorption tube could be heated uniformly to about 240°C. When the furnace had to be heated to still higher temperatures, additional furnaces, F_3, were added on the both ends. They were used to compensate the heat loss of the ends to the surroundings.

The furnace F_2 was made by simply winding the resistance wire around the side tube protected by asbestos paper and mica. The furnaces F_3 were made by first winding the heating wire on a cylinder covered with asbestos then putting it inside another bigger cylinder forming a very compact heating unit.

The temperature of the absorption tube was measured by an alumel-chromel thermocouple. The hot junction was fastened tightly by a steel ribbon on the pressure tube at the portion T shown in Fig. 3.

The whole furnace was placed in a box full of asbestos powder. As the side tube had to be put below the absorption tube [12], the whole box was laid on a wooden table with a big hole at the center. In this way the cold gas in the side tube will not flow into the absorption tube on account of its higher density than that of the hot gas in the main tube.

Water coolings were applied immediately outside of the heating box to cool the side tube. The upper one composed of two semi-cylindrical vessels as shown in Fig 4. They could be applied and taken off much more conveniently than the lower water cooling copper tubings. The function of the water coolings was not only to keep the cross tube and the needle valves, V, cooled, but also to condense the rubidium vapor if it escaped out of the absorption tube A, when foreign gas was being inserted into the tube from the value V_1, or when the tube was cooling down[13]. The ends of the absorption tube A were closed tightly by pressing the Mg O windows on the sharp edges of the tube ends.

---

(12) Otherwise if the side-tube was pointed upward, as soon as the hot gas coming from the main tube was cooled, it would be displaced by new supply of hot gas. So there would be a convection and the side-tube would be too hot.

(13) When the tube was cooling down the foreign gas outside of the absorption tube A would be cold first resulting in a higher pressure inside the tube A. So the foreign gas would carry the alkali vapor out of the tube A.

The joint between the inner side-tube and the tube A was also very tight, so the only way for the gas to flow from the inner absorption tube A to the pressure tube was to flow through the opening, J, in Fig 1. So this arrangement served to give a connection between the outer and the inner tubes for the foreign gas, not for the alkali vapor.

(c) The needle value, the pressure gages, etc.

Three needle volves, V_1, V_2, V_3, were used. V_1 led to the pressure tank containing foreign gas; V_2 was connected to the pressure gage, and V_3 joined the high vacuum pump.

On the value, V_1, the nut joining the thin copper tubing which led to the pressure tank of foreign gas and V_1 was shown on the Fig. 3. Between V_1 and the pressure tank was the thick walled copper tubing and a condensing spiral as shown in Fig. 5. The condensing spiral was made of thick walled copper tubing about $\frac{1}{2}$ inch outside diameter. It was used to fill back the argon into the tank after the experiment was through. When condensing spiral was dipped into liquid air, with value V_1 opened and the tank closed, the argon gas was condensed and crystallized.

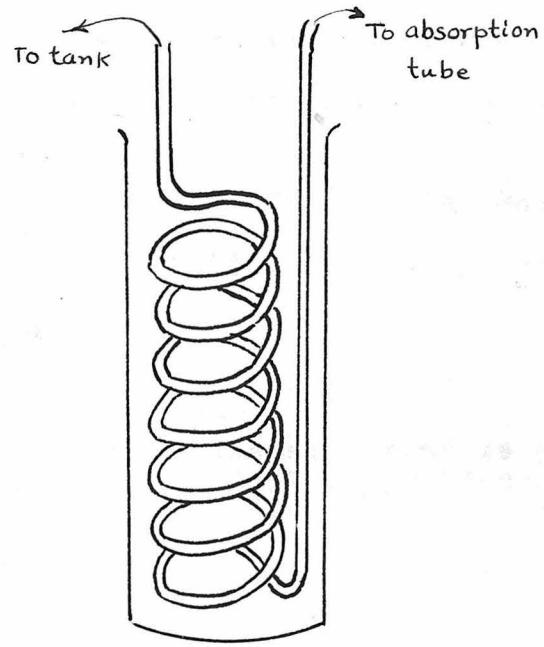

Fig. 5 The cooling spiral

Consequently the pipe was filled up with solid argon. Then V_1 was closed and the tank valve was opened. By lifting slowly the condensing spiral out of the liquid air bottle the spiral was warmed up. Then argon condensed at the top of the spiral vaporized first and went back to the tank as soon as the pressure was raised high enough. Care must be taken to connect the ends of the spiral in the way shown in the figure. If the terminals were otherwise connected; and if the spiral were warmed up, the boiled argon could hardly go through the lower (cooler) part of the spiral which would be closed by the solid argon. So very probably a dangerously high pressure could be built up in the tubing.

Three pressure gages were used. They served to measure the pressure in three ranges ___ 1 - 300 lbs, 1 - 600 lbs, and 1 to 3000 lbs. These gages were calibrated by means of a standard pressure gage [14]. The first two gages were calibrated to read a pressure accurate to 1 lb, while the third one could read to 10 lbs.

(d) The Foreign Gases

Helium, argon and hydrogen were used as foreign gases.

---

(14) The standard pressure gage was situated in Mechanical Engineering Building, Caltech. Thanks are due to Dr. B.H.Sage for his permission to use the apparatus.

The helium gas [15] was obtained originally from evaporation of liquid helium, and was once more purified by absorption method to eliminate contaminations by the sealing liquid during storage. The total impurity at the source is estimated to be smaller than .01% The small trace of impurity would be hydrogen.

The argon tank was supplied by the Ohio Chemical & Mfg. Co. Cleveland, Ohio. The purity was 99.6 % The impurity would be nitrogen.

The hydrogen tank was supplied by the Cryogenic Laboratory of this Institute. The gas was claimed to be about 99.5 % pure.

The remaining parts of the apparatus such as the tungsten light source, the preparation of metallic rubidium, and photographic photometrical parts are all the same as those in the first research, and thus are omitted here.

The dimensions of apparatus such as the thickness of tube walls, of the copper tubings and of Kovar cones, the thread on the window frames, the thickness of the pyrex glass windows etc. were carefully designed. The factor of safety was about 5.

---

(15) Thanks are due to Prof. A. Goetz, the director of the cryogenic laboratory of this Institute, for his most generous permission and help to use his (precious) pure helium.

Before using the apparatus, it was put outside the laboratory and was tested for pressure. During experiment the absorption tube was first cleaned and the contained gas in the tube wall was removed by long pumping and heating. Then metallic rubidium was inserted into the absorption tube A in a current of nitrogen. The tube was then pumped again immediately. The absorption spectrum of rubidium was taken when the pure foreign gas was admitted into the tube and the tube was heated to a certain temperature. The temperature was so adjusted at each pressure of the foreign gas so that the absorption was less than the total in the center of the resonance lines in order that true line contours would be registered. To calibrate the density gradations in the absorption lines, the plate (Eastman Kodak Type I-R) was calibrated by a step weakener placed in the plate holder just on one side of each absorption line as shown in Fig. 10. An iron arc spectrum was supperposed on both sides of the mean exposure as a comparison.

The method of measuring the broadening of the lines was in general the same as before. Microphotometer curves were recorded on bromide paper 43x12 cm^2 in a drum camera. From the step weakener marks, deflections vs. density curves were given for each plate. Then the true line contours (density vs. wave-length) were plotted, Figs. 12. Absolute absorption coefficient could easily be calculated from the values of

the density, D, and the well determined length of the optical path in the absorption vapor. The half width which is the frequency range in which the absorption corfficient is a half of its maximum, could be read off directly. The asymmetry of each line was both expressed in terms of the ratio of the "red" half to the "violet" half of the half-width and in terms of the ratio of the respective areas under the red and the violet halves of the absorption contour, as measured by a Polar planimeter.

The amount of displacement was determined from the microphotometer curve with a scratch made at convenient positions. All results were given in the next chapter.

III RESULTS AND DISCUSSION

(a) Broadening:

The half width of the Rb resonance lines broadened by different concentrations of helium, argon and hydrogen are tabulated in Table II. In the first three columns are given the plate number, the pressure in atmosphere and the temperature in absolute scale of the foreign gas employed. In the fourth column the concentrations of the perturbing gas are expressed in terms of "relative density," the unit being the density of the same quantity of a foreign gas as that used in the experiment, but at $0^{\circ}C$ and 1 atmosphere. The half widths are given both in terms of Angström units and in wave number. In Figs. 6 and 7 are given the plots of the values. The half widths turns out to be linearly proportional to the relative densities of these gases, indicating the predominance of velocity broadening even in this high pressure range. The slope of these curves are .735 cm^{-1} and .594 cm^{-1} per unit relative density of helium for $^2P_{3/2}$ and $^2P_{\frac{1}{2}}$ components respecitively, and the corresponding values for argon are .855 cm^{-1} and .627 cm^{-1} per unit relative density.

The degree of accuracy of the determinations depends on the experimental conditions. For lower pressure the lines were narrow and the graininess of the plate (Type I-R) caused appreciable irregularities in the microphotometer curves, the precision in the determination of both the absorption maximum and the line contour were appreciably affected, while for high

Table II. The broadening of the resonance lines of Rb produced by He, A and H_2

Plate No.	P Atmos.	T °K	Relative density	Half width (λ7947) Å	Half width (λ7947) cm^{-1}	Half width (λ7800) A	Half width (λ7800) cm^{-1}
			(a) Rubidium/Helium				
He 14	3.95	447	2.41	1.019	1.613	1.086	1.785
He 13	8.98	455	5.39	1.937	3.067	2.242	3.685
He 4	20.48	461	12.13	4.966	7.863	5.582	9.175
He 5	41.10	463.5	24.21	10.707	16.953	10.389	17.075
He 12	77.29	569±2	37.08	13.730	21.740	16.916	27.803
He 11	96.62	579.5	45.52	16.916	27.803	20.205	33.210
He 9	98.79	581.5	46.36			20.968	34.463
			(b) Rubidium/Argon				
Ar 1	2.72	440±2	1.69	.818	1.295	.738	1.213
Ar 2	6.12	515±1	3.24	1.740	2.755	1.920	3.156
Ar 3	10.21	517.5	5.39	2.128	3.369	2.080	3.419
Ar 4	19.94	527±6	10.33	4.562	7.223	4.437	7.293
Ar 5	41.16	552±1	20.36	9.535	15.098	11.839	19.459
Ar 6	71.44	569±7	34.28	14.302	22.646	19.706	32.389
Ar 7	85.73	576.0	40.63	15.784	24.992	20.977	34.478
Ar 8	97.96	576	46.44	17.680	27.995	23.738	39.016
			(c) Rubidium/Hydrogen				
H 2	20.00	462	11.82	4.53	7.73	6.24	10.256

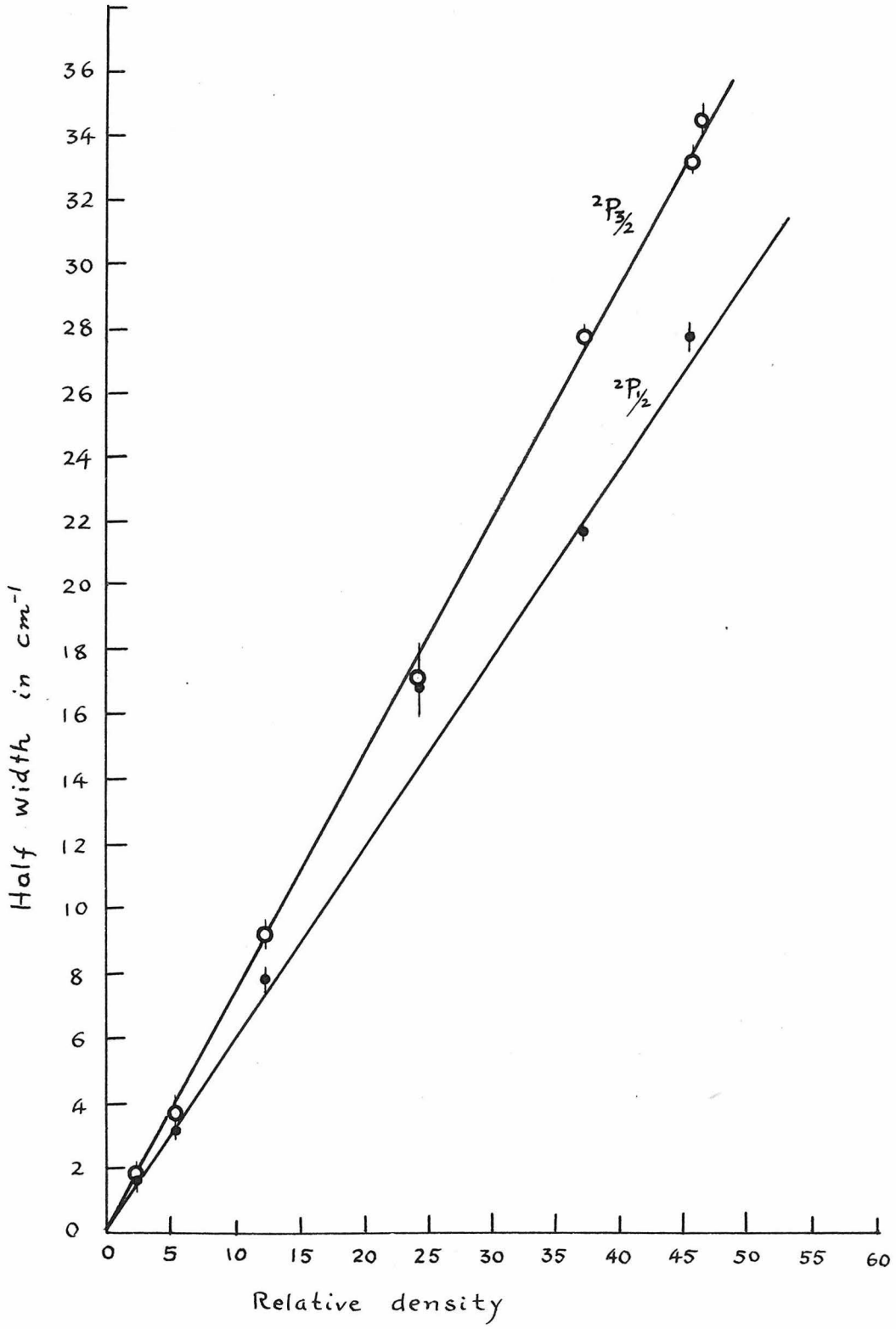

Fig. 6. Half width vs relative density curve for helium

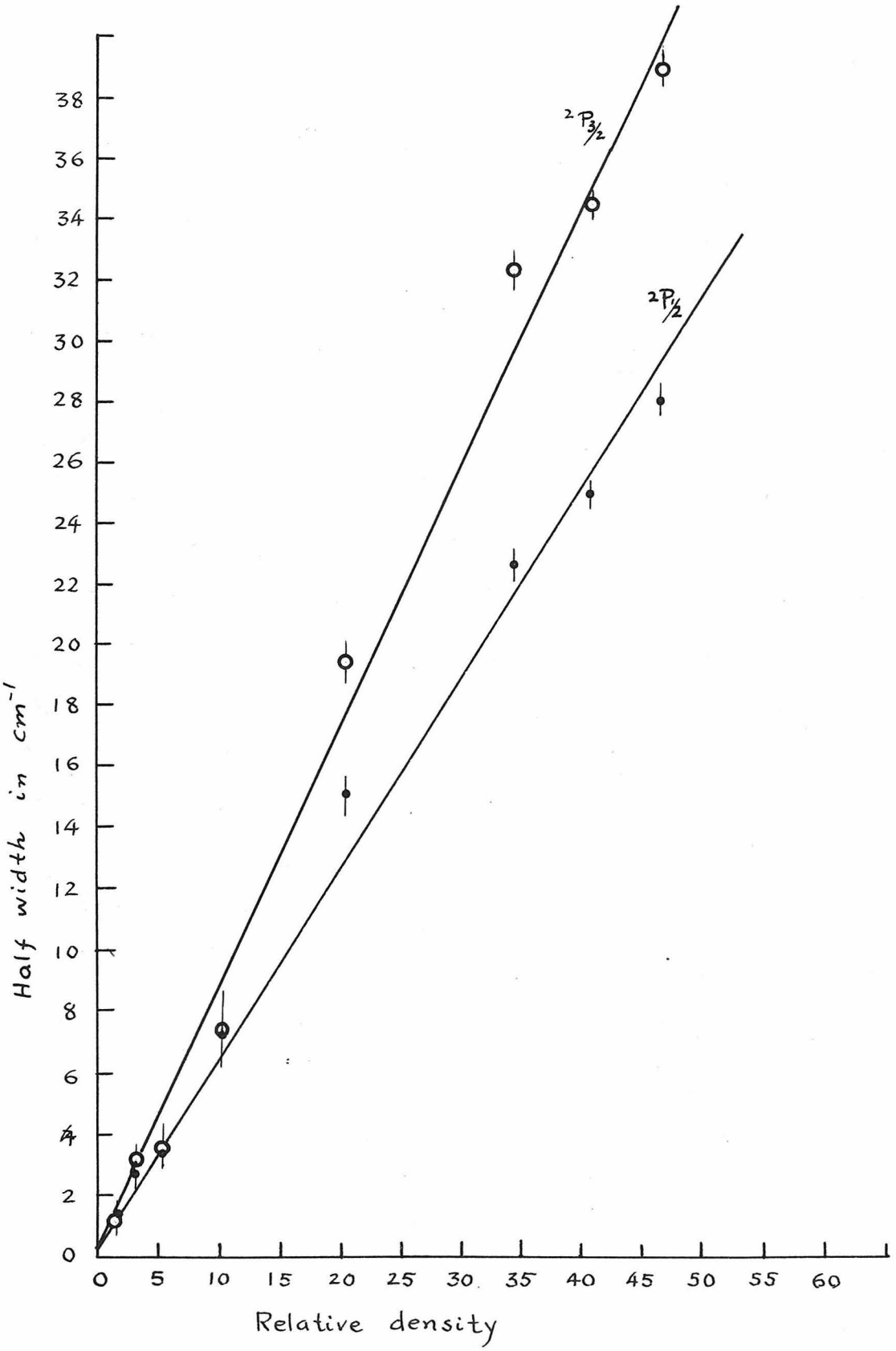

Fig. 7 Half width vs. relative density curve for argon

pressures the lines were so highly broadened that the irregularity could be easily smoothed out without affecting the true shape of the line contaur. Also when the temperature of the absorption tube was not suitably adjusted so that the absorption at the center of the resonances lines was too high or too low, the accuracy was naturally lowered. The degree of precision was estimated and is shown in Figs. 6 and 7.

It is to be noted that the broadening by argon is greater than that by helium and the broadening of the shorter wave-length component is slightly greater than that of the longer wave-length one for both gases.

Watson and Margenau [16] and Hull [17] have shown in their results for sodium (with H_2, N_2 and A) and potassium (with N_2 and A) that there is no significant difference between the half widths of the doublet components for resonance lines and also for the second doublet of the potassium principal series. But petermann [18] found that the blue Cs doublet and the corresponding potassium doublet show about 20 percent greater broadening for the shorter wave-length component when broadened by hydrogen. Ny and the author [19]

---

(16) H. Margenau and W.W. Watson, Phys. Rev. 44, 92, 44,1939.
(17) G.F. Hull, Phys. Rev. 50, 1148, 1936.
(18) Petermann, Zeits. F. Physik 87, 96, 1933.
(19) Ny Tsi-Ze' and Ch'en Shang-yi,Phys. Rev. 52,1158,1937.

found that for helium and neon the half widths of the $^2P_{\frac{1}{2}}$ component of the second doublet of Rb principal series is greater than that of the $^2P_{3/2}$ component, while for argon the half widths of the $^2P_{\frac{1}{2}}$ component is slightly greater. In the present research the results for argon are in harmony with those of the author's former experiment for the second member of Rb principal weries. The difference between the half widths of the doublet components detected both by the former and by the present researches suggests again that the perturbing effect of neighbouring atoms (similar or dissimilar) may be different for different j-values.

It is interesting to note that according to Margenau's theory, the half width should be proportional to the relative density of the perturbing gas as long as the velocity breadth is the predominant one, the statistical width grows with the square of the relative density. A point will be reached at which the two are equal, and a curvature in the graph of $\Delta\nu_{\frac{1}{2}}$ vs. n should set in indicating a change to the statistical n^2-law as we pass from this point to higher relative densities. This point occurs when $\Delta\nu_{\frac{1}{2}} \approx \pi\lambda_\alpha^2$

Where $\lambda_\alpha = \frac{2}{3}\pi\alpha^{\frac{1}{2}}$ n where α is an interaction constant. The departure from the linear relationship has been confirmed by Margenau for K resonance lines. But Füchtbauer, Joos, and Dinklacker [20] have measured the broadening of Hg λ2537

(20) Füchtbauer, Joos, and Dinkelacker, Ann. d. Physik, 71, 204, 1923.

produced by pressures up to 50 atmospheres of foreign gases. They found the width to vary linearly with the density of the perturbing gas. In the present work also, no deviation from the linear law has been observed for the rubidium resonance lines for concentrations of He and A up to 100 atmospheres.

(b) Asymmetry

So far there is no generally accepted satisfactory way to figure out the asymmetry of the broadened lines. In Table III are given the values both in the ratios of the red "half" to the blue"half" of the half-widths as listed in the third and fifth columns represented by (1) and in the ratios of the areas under the red half to these under the violet half of the line contour as represented by (2) in the table. A value which is unity indicates a symmetrically broadened line, a value smaller than unity a violet asymmetry, and a value large than unity a red asymmetry.

Helium produces a violet asymmetry, while argon a red asymmetry. The degree of asymmetry increases as the concentration of helium or argon increases. For helium the degree of asymmetry is a little greater for the longer wavelength component, while for argon the degree of asymmetry for the shorter wavelength component is greater. For argon the degree of asymmetry first increases very rapidly with the increase of concentration, then attains a weak maximum around relative density 10, finally the asymmetry drops slightly to a nearly constant value. The degree of asymmetry produced by helium is comparatively much lower than that produced by argon. The asymmetry was small when the relative density was below 10, but increased gradually with the increase of concentration. The asymmetry produced by the hydrogen is quite small.

Table III. The asymmetry of the broadened Rb resonance lines produced by He, A and H_2

Plate No.	Relative density	Asymmetry (λ7947) (1)	(λ7947) (2)	Asymmetry (λ7800) (1)	(λ7800) (2)
	(a)	Rubidium/Helium			
He 14	2.41	0.95	0.911	1.00	0.988
He 13	5.39	0.98	0.967	1.01	0.990
He 4	12.13	0.97	0.843	0.98	0.961
He 5	24.21	0.78	0.772	0.88	0.874
He 12	37.08	0.83	0.782	0.90	0.832
He 11	45.52	0.86	0.777	0.99	0.748
He 9	46.36				
	(b)	Rubidium/Argon			
Ar 1	1.69	1.07	1.128	1.41	1.538
Ar 2	3.24	1.39	1.588	1.50	1.654
Ar 3	5.39	1.56	1.661	1.50	1.702
Ar 4	10.33	1.79	1.975	1.71	1.912
Ar 5	20.36	1.42	1.387	1.60	1.641
Ar 6	34.28	1.38	1.374	1.80	1.825
Ar 7	40.63	1.33	1.395	1.58	1.658
Ar 8	46.44	1.36	1.352	1.63	1.568
	(c)	Rubidium/Hydrogen			
H 2	11.82	1.18		1.00	

The values listed under the columns numbered (1) and (2) permit interesting comparison of the two ways of describing the nature of the asymmetry of the line contours. The first way (the ratios of the halves of the half-widths as represented by (1))gives in general the asymmetry at nearly the central portion of the line. The asymmetry at the far wings is not given. While the second way (the ratios of the areas under the line contour as represented by (2)) is a more sensitive way of measuring the asymmetry for the asymmetry of the line would effect the area more conspicuously than the half width. The asymmeties were most pronounced near the base of the line. The values of the last two columns for helium in table III give a good illustration.

Although three figures are recorded in expressing the degree of asymmetry, the last figure has very little significance as regards the accuracy of measurement. The chief source of error is in the planimetric measurement near the end of the wings. The wing streched very far on both sides of the wings especially the side which showed asymmetry, a little error in traceing the line contour would effect the area by a considerable amount.

(c) Shift

The displacement of the central maxima of the Rb resonance lines produced by helium and argon are given in Table IV , and are plotted in Figs. 8 and 9. Argon produce a greater shift than helium. The former produces a strong red shift, while the latter a violet shift. For both gases the shift of the $^2P_{\frac{1}{2}}$ (λ7947) component is greater than that of the $^2P_{1\frac{1}{2}}$ (λ7800) component. This phenomenon is shown very obviously in Figs. 10 and 11.

In Figs. 10 and 11 are given a direct comparison of the positions of the Rb resonance lines, with and without the effects of foreign gases. Fig. 10 (a) and Fig. 11 (a) are the spectra taken with the absorption tube containing pure rubidium vapor at very low pressure (10^{-3} mm. Hg), Figs. 10 (b) and 11(b) are those taken when the pure Rb vapor pressure was increased to 4 mm. Hg, and Figs. 8 (c) and 9 (c) are the spectra taken when foreign gases were introduced. As pointed out in the first article, and also shown here, the shift of Rb resonance lines due to the pressure of its own vapor is very small. But the large shift of the lines produced by foreign gases is strikingly illustrated. It is well known that the shift of the resonance lines produced by foreign gases is smallest among the series lines. The shift vs. series members curve (21) shows

---

(21) For instance,
Füchtbauer, Schülz and Brandt, Z.f.Physik. 90, 403, 1934.
Ny Tsi-Ze and Ch'en Shang-yi, Phys. Rev. 51, 567,1937; 54, 1045, 1938.

Table IV. The displacement of the resonance lines of Rb produced by He, A and H_2

Plate No.	Relative density	Shift (λ7947) Å	Shift (λ7947) cm^{-1}	Shift (λ7800) Å	Shift (λ7800) cm^{-1}
		Rubidium/Helium			
		(violet)	(violet)	(violet)	(violet)
He 14	2.41	0.25	0.39	0.12	0.19
He 13	5.39	1.17	1.85	0.58	0.95
He 4	12.13	1.83	2.89	0.92	1.52
He 5	24.21	3.64	5.76	1.37	2.26
He 12	37.08	4.77	7.54	1.59	2.62
He 11	45.52	6.88	10.88	2.68	4.40
		Rubidium/Argon			
		(red)	(red)	(red)	(red)
Ar 1	1.69	0.52	0.82	0.22	0.36
Ar 2	3.24	0.65	1.03	0.29	0.48
Ar 3	5.39	1.07	1.69	0.81	1.33
Ar 4	10.33	2.92	4.63	2.43	3.99
Ar 5	20.36	6.96	11.01	5.86	9.64
Ar 6	34.28	12.78	20.23	11.77	19.63
Ar 7	40.63	15.26	24.17	15.81	26.04
Ar 8	46.44	18.47	29.90	18.16	29.85
		Rubidium/Hydrogen			
		(violet)	(violet)	(red)	(red)
H 1	2.07	0.83	1.32	0.81	1.33
H 2	11.82	1.03	1.63	0.98	1.61

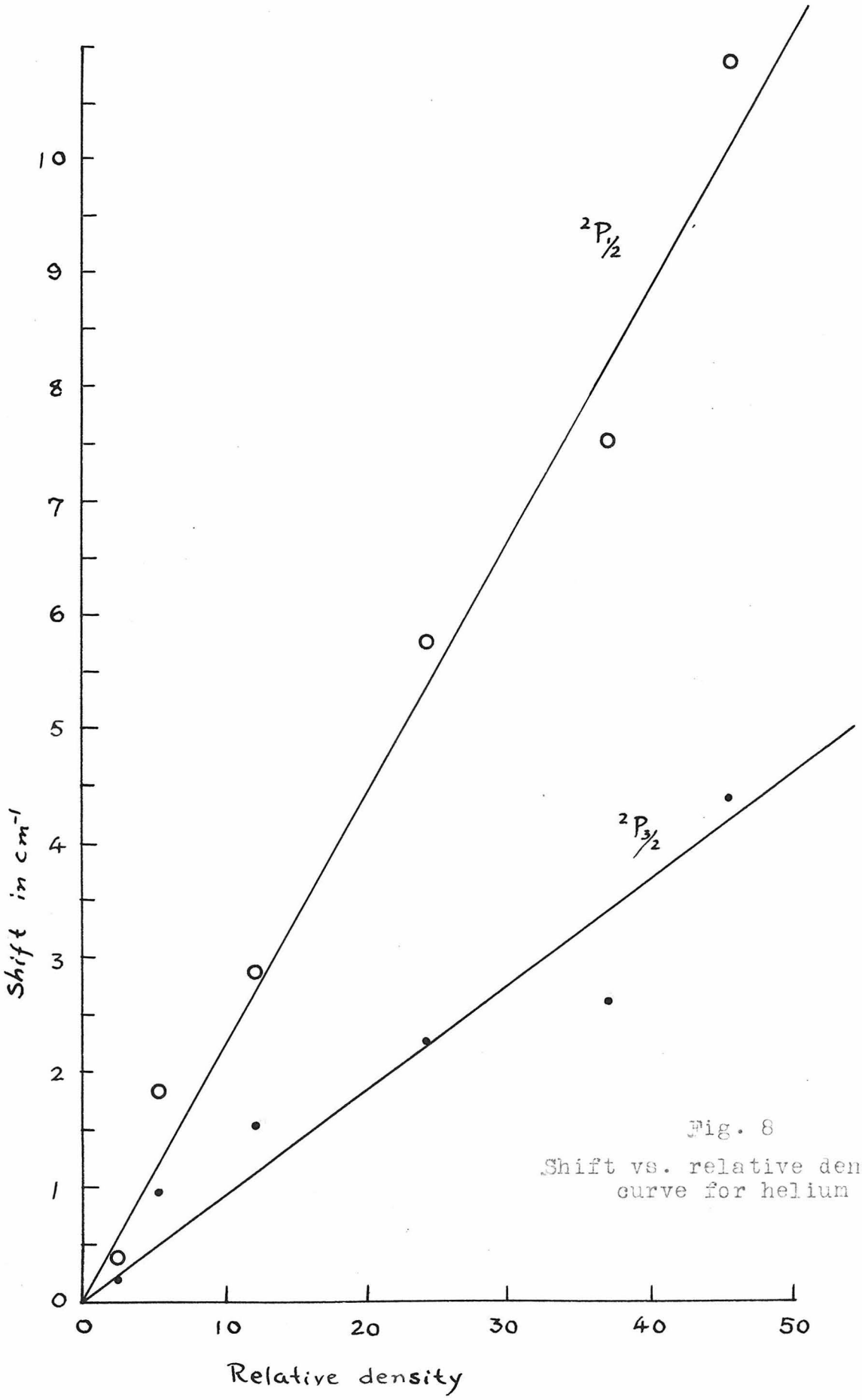

Fig. 8

Shift vs. relative density curve for helium

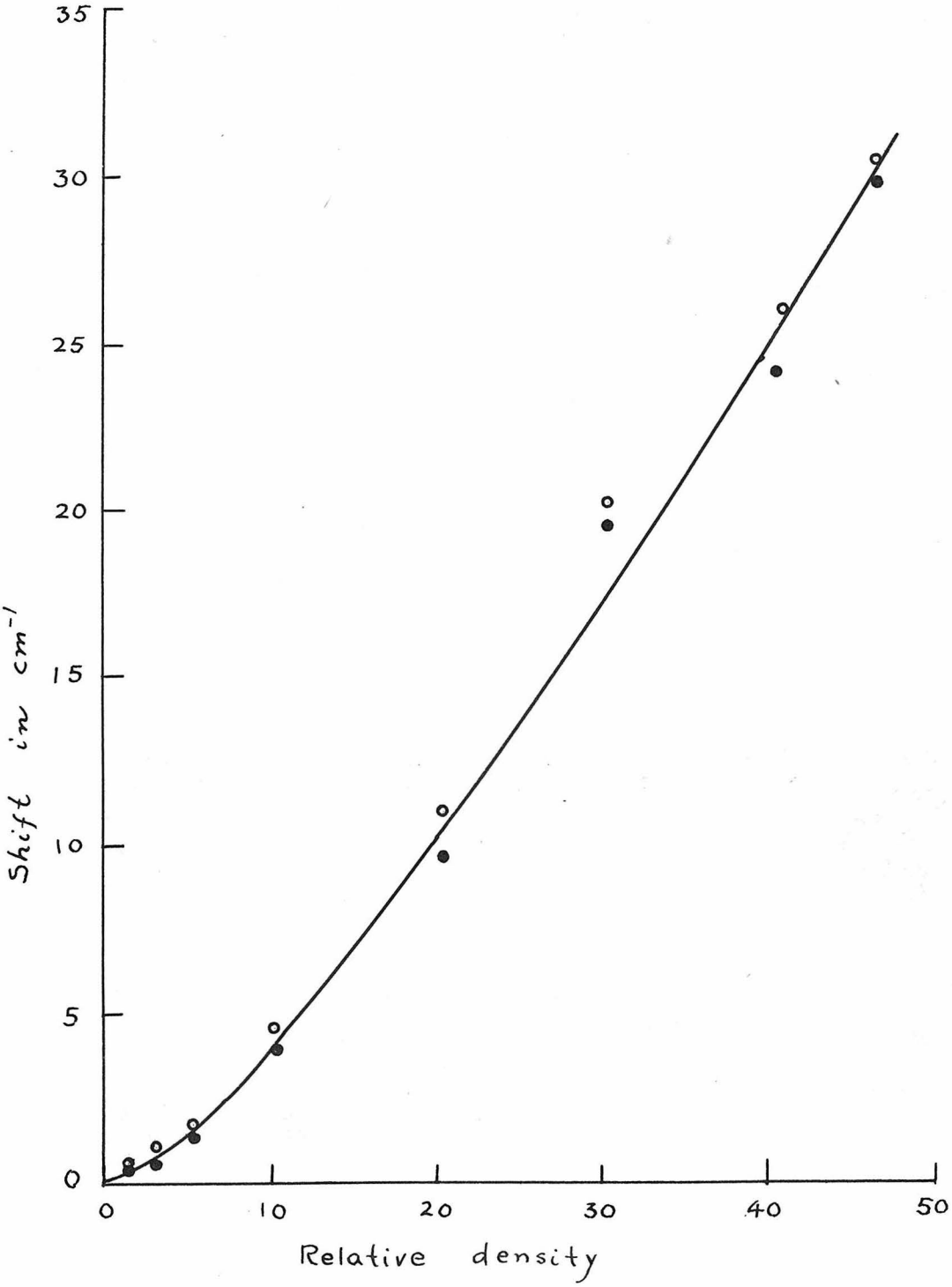

Fig. 9 Shift vs. relative density curve for argon

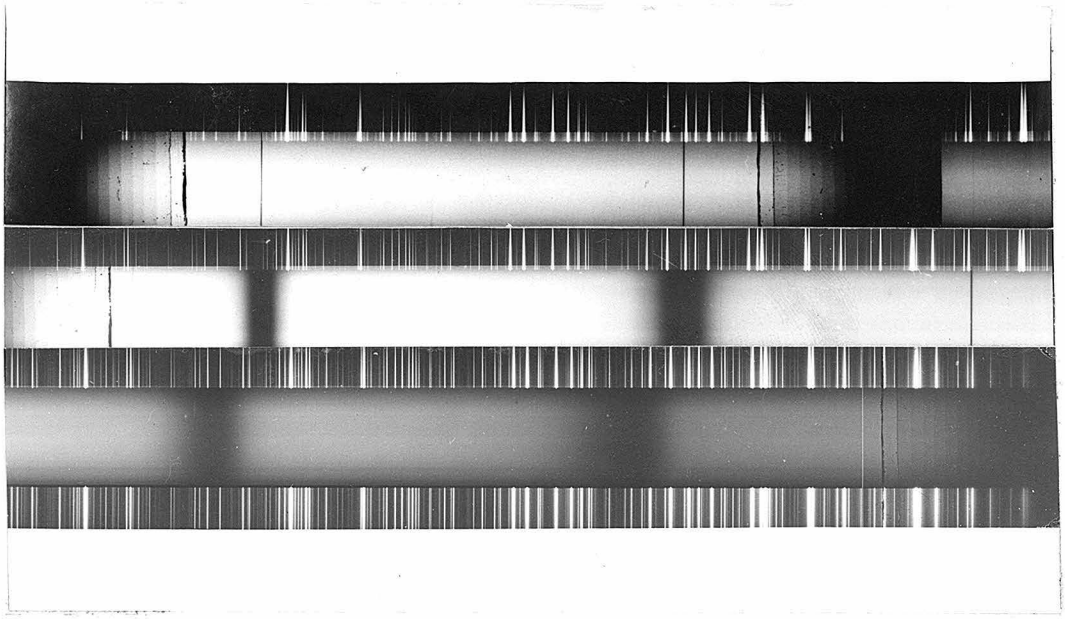

Fig. 10 Positions of rubidium resonance lines

(a) Under 10^{-3} mm. pressure pure vapor (T= 180 C)
(b) Under 4 mm. Hg pressure pure vapor (T= 347 C)
(c) Under 97.98 atmospheres argon (T= 303 C)

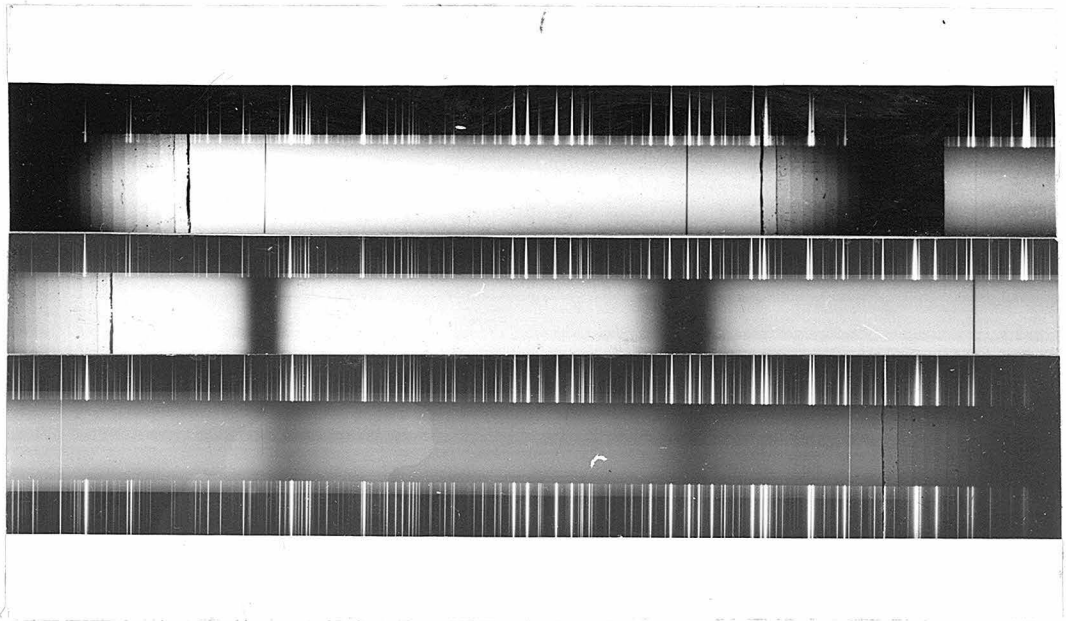

Fig. 11. Positions of rubidium resonance lines

(a) Under 10^{-3} mm. pressure pure vapor (T= 180 C)
(b) Under 4 mm. Hg. pressure pure vapor (T= 347 C)
(C) Under 96.62 atmospheres helium (T= 306.5 C)

that the shift first increases strongly with the ordinal number of the lines in the series, then attains a weak maximum and finally approaches a constant value for the lines near the limit of the series. Thus it is easy to imagine that under so big a foreign gas pressure (100 atmospheres) the shift for higher series members would be as big as one hundred Angstrom units. Hydrogen produce a violet shift on the longer wave-length component and a red shift on shorter wave-length component of the Rb resonance lines.

It is to be noted from Figs. 8 and 9 that for helium the shift appears to be proportional to the relative density, while for argon there is noticeable departure from linear relation ship. For argon the shifts for the two doublet components are very nearly the same, while for helium the shift of the longer wave-length component is about twice as great as for the shorter wave-length component. (see also Figs. 10 and 11)

The difference of shifts of the two components has already been pointed out by Margenau Watson & Hull [22] in their experiments on effects of nitrogen and argon on potassium resonance lines and also by Ny and the author[23] in their experiment on the effects of rare gases on the second member of Rb absorption series.

---

(22) Margenau and Watson. Phys. Rev. 44, 92, 1933 Hull Phys. Rev. 50, 1148, 1936.
(23) Ny Tsi-Ze and Ch'en Shang-yi, Phys. Rev. 52, 1158, 1937.

The relation between the shift and the relative density is still an unsolved problem. Some theories have identified the shift with the mean of the frequency distributions, $\overline{(\nu - \nu_0)}$. It will be always strictly proportional to the relative density and depends in sensitive manner on the distance of closest approch. But Kuhn [24] pointed out that the meassured shift is not the mean but the displacement of the maximum. So the shift should be proportional to the square of the density of the gas and is largely independent of the distance of closest approach. In fact both the linear and the quadratic relations were observed. In the present case the shift of the lines produced by helium is in general linearly proportional to the relative density, but for argon the relation between shift and relative densities obeys in general the 3/2 power relationship. The accuracy of locating the positions of the maxima of these lines was estimated, the greatest possible error should not be more than 2% [25] although one could regard that pressure region as corresponding to $\Delta \approx \pi\lambda_\alpha$ [26], in which the linear law gradually changes into the square law, yet further theoretical confirmation of the existence of this change seems very desirable.

---

(24) H. Kuhn, Phys. Rev. 52, 133, 1937.
(25) As estimated from the measurements of the magnification ratios on the microphotometer, the location of the line maximum, the inaccurcy of measurement on the scratch made on the plate, and the density readings of foreign gases
(26) Margenau and Watson, Rev. Mod. Phys, 8, 47, 1936.

In order to approach as much as possible the theoretical assumptions it is desirable to use low pressures and high atomic weight so that the influence of atomic motion is eliminted. But due to the wide spread of the lines [27] the temperature of the absorption tube had to be raised to too high a value so that the absorption of the line could be easily meassurable.

---

(27) Since the area under the absorption line contour depends on the number of absorpting atoms, the line will be diffused when it is broadened.

(d) The areas under the absorption line contours and the evaluation of f-values and transition probabilities

The amount of the total absorption, i.e. $\int_0^\infty (n\kappa)\, d\nu$, for each line was determined. $n\kappa$ is the electron theory absorption coefficient which is connected with the usual absorption coefficient by the relation

$$(n\kappa) = K_\nu$$

So that

$$n\kappa = \frac{\lambda}{4\pi l} \log I_0/I$$

where l is the absorption path length. Therefore the value of the integral $\int_0^\infty (n\kappa)\, d\nu$ can be computed from the area under the line contour ($\log_{10} I_0/I$ vs. $\delta\lambda$) curve by multiplying it by a factor $2.303 \times c / 4\pi l\lambda$, where λ is taken as the wave-length of the central maximum. In the present work the line contours were plotted with $\log_{10} I_0/I$ or D as ordinate and the distance in mm. from the central maximum of the microphotometer curve as abscissa, as shown in Figs. 12. The areas A under the line contour were measured by a planimeter in cm^2, 1 cm in ordinate corresponding to .02 in density and 1 cm in abscissa corresponding to 26.4/ nm Å where m is the magnification ratio of the microphotometer trace, and n the magnification ratio on the graph. So

$$\int_0^\infty (n\kappa)\, d\nu = \frac{2.303}{4\pi l\lambda} \times 3 \times 10^{10} \int_0^\infty \log_{10} I_0/I\ \delta\lambda$$

$$= \frac{2.303}{4\pi l\lambda} \times 3 \times 10^{10}\ \frac{26.4 \times 10^{-8}}{n\ m\ \ .02} \times A$$

where l = 25.6 cms.; m = 19.04 and 6.71 or 6.65 depending upon the ratios used and the thickness of the bromide paper.

Table V. The f-values of rubidium resonance lines under different pressures of foreign gases

Plate No.	T K	p mm. Hg	n	R. D.	f_s	f_l
			(a) Rubidium/ helium			
He 14	447	1.25×10^{-2}	2.71×10^{14}	2.41	.780	.467
He 13	455	1.79×10^{-2}	3.81×10^{14}	5.39	.614	.323
He 4	461	2.32×10^{-2}	4.88×10^{14}	12.13	.463	.253
He 5	463.5	2.58×10^{-2}	5.404×10^{14}	24.21	.307	.186
He 12	569±2	1.00	1.70×10^{16}	37.08	.202	.152
He 11	579.5	1.337	2.238×10^{16}	45.52	.0884	.0742
			(b) Rubidium/ argon			
Ar 1	440±2	9.00×10^{-3}	1.98×10^{14}	1.69	.595	.281
Ar 2	515±1	1.58×10^{-1}	1.98×10^{15}	3.24	.582	.301
Ar 3	517.5	2.023×10^{-1}	3.792×10^{15}	5.39	.503	.264
Ar 4	527±6	2.78×10^{-1}	5.12×10^{15}	10.33	.511	.253
Ar 5	552±1	6.08×10^{-1}	1.07×10^{16}	20.36	.378	.220
Ar 6	569±7	1.00	1.70×10^{16}	34.28	.253	.172
Ar 7	576.0	1.214	2.044×10^{16}	40.63	.304	.194
Ar 8	576	1.214	2.04×10^{16}	46.44	.305	.197

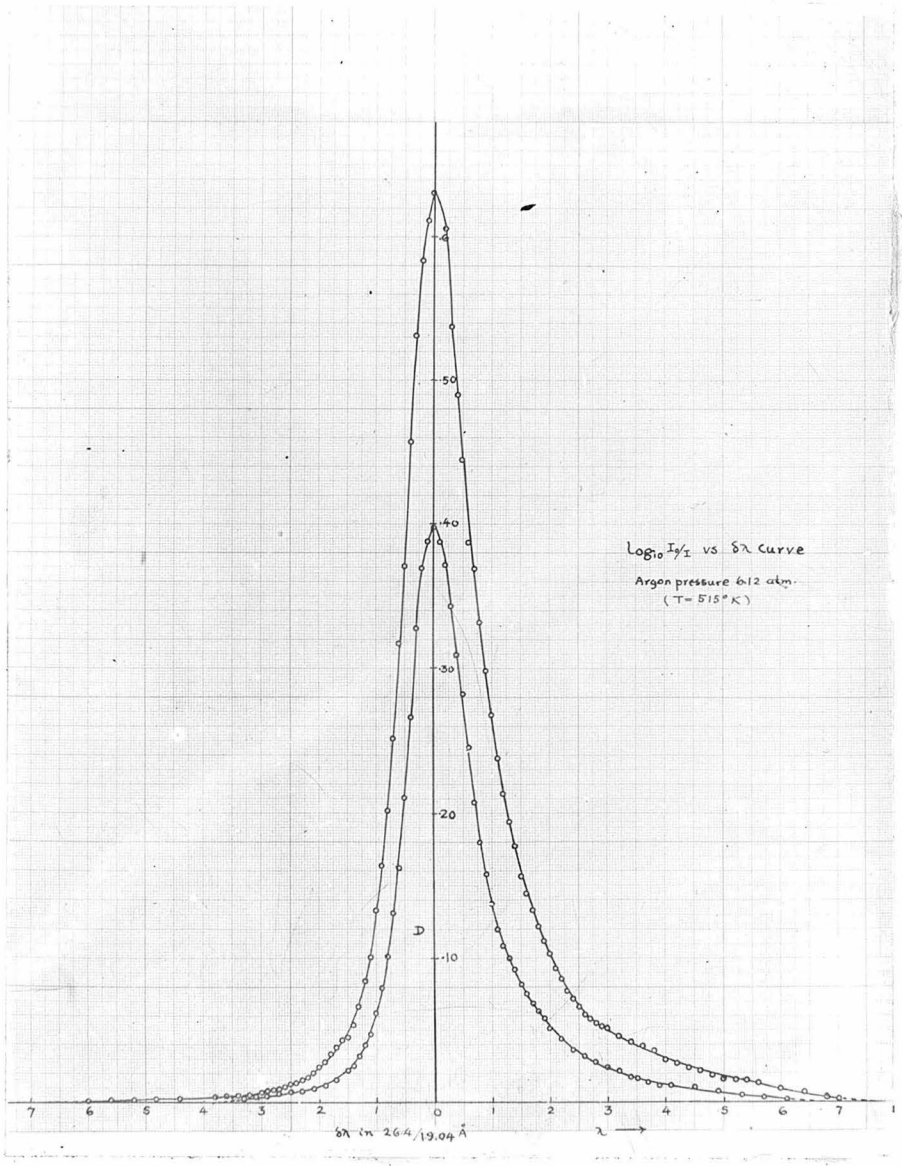
$\log_{10} I_0/I$ vs $\delta\lambda$ curve
Argon pressure 6.12 atm.
(T = 515° K)
D
.50
.40
.30
.20
.10
7 6 5 4 3 2 1 0 1 2 3 4 5 6 7
$\delta\lambda$ in 264/19.04 Å
$\lambda \rightarrow$

Fig 12 a

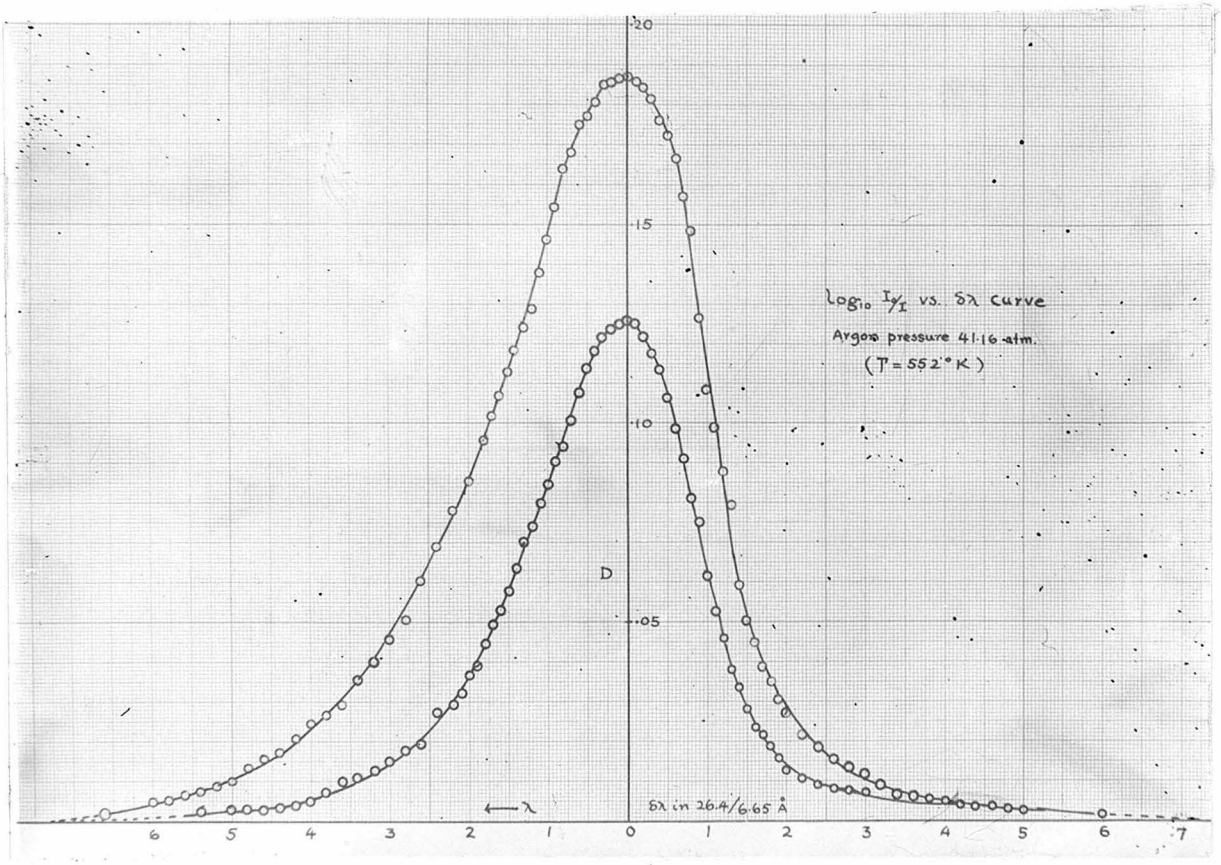
Log10 I/I vs. δλ Curve
Argon pressure 41.16 atm.
(T = 552° K)
.20
.15
.10
.05
D
← λ
δλ in 26.4/6.65 Å
6 5 4 3 2 1 0 1 2 3 4 5 6 7

Fig. 12 b

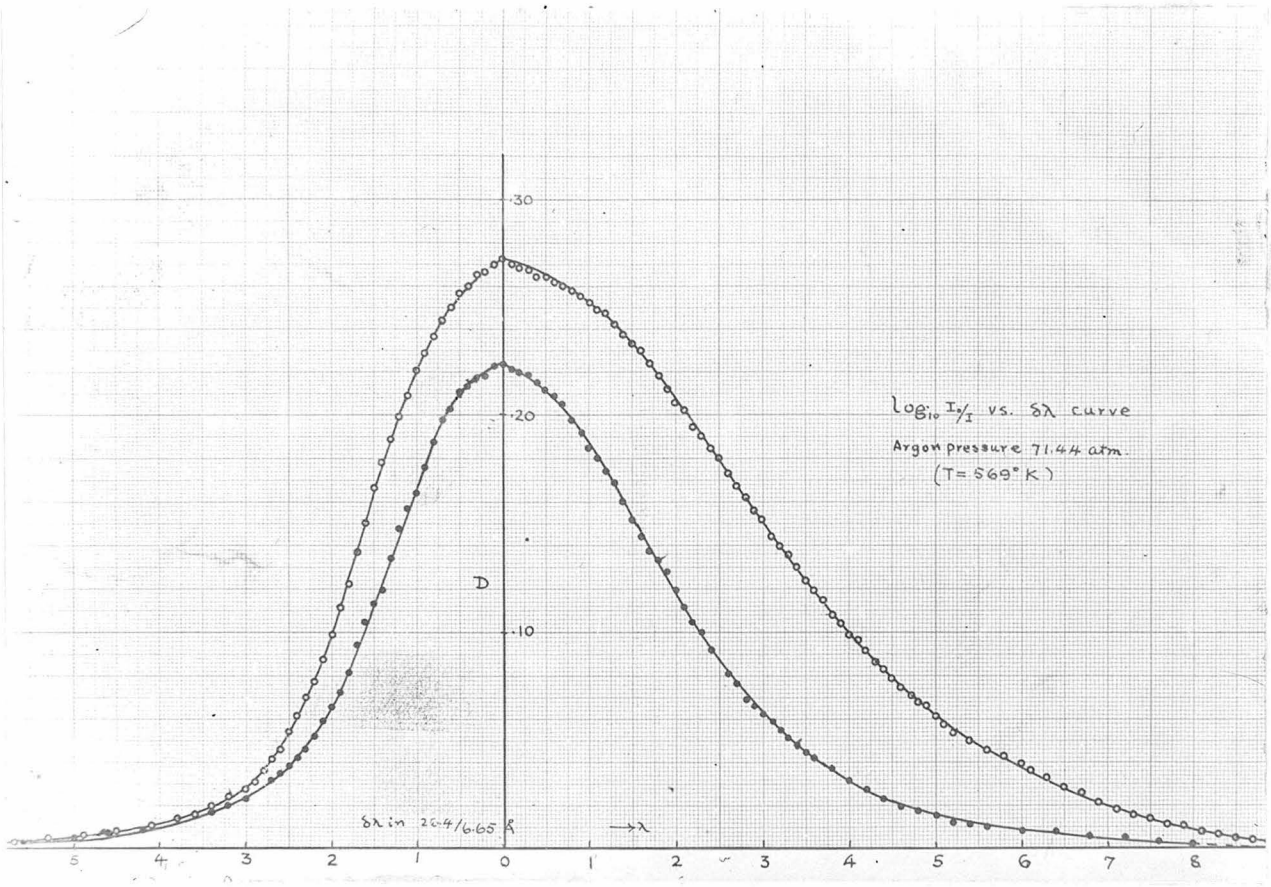
log10 I'/I vs. δλ curve
Argon pressure 71.44 atm
(T = 569° K)
30
20
10
D
δλ in 26.4/6.65 Å
→λ
5
4
3
2
1
0
1
2
3
4
5
6
7
8

Fig. 12 c

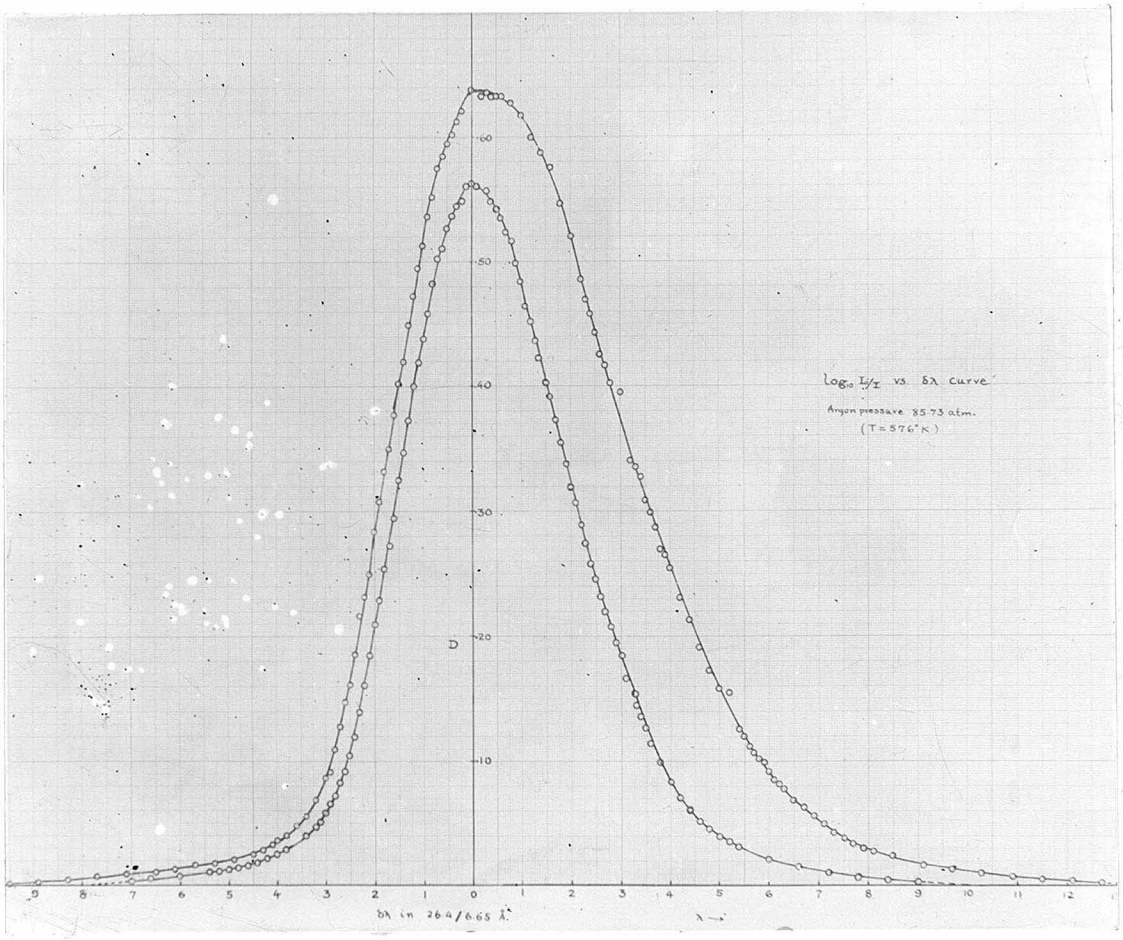
log₀ I₀/I vs. δλ curve
Argon pressure 85.73 atm.
(T = 576°K)
D
δλ in 264/6.65 Å
λ →

Fig. 12 d

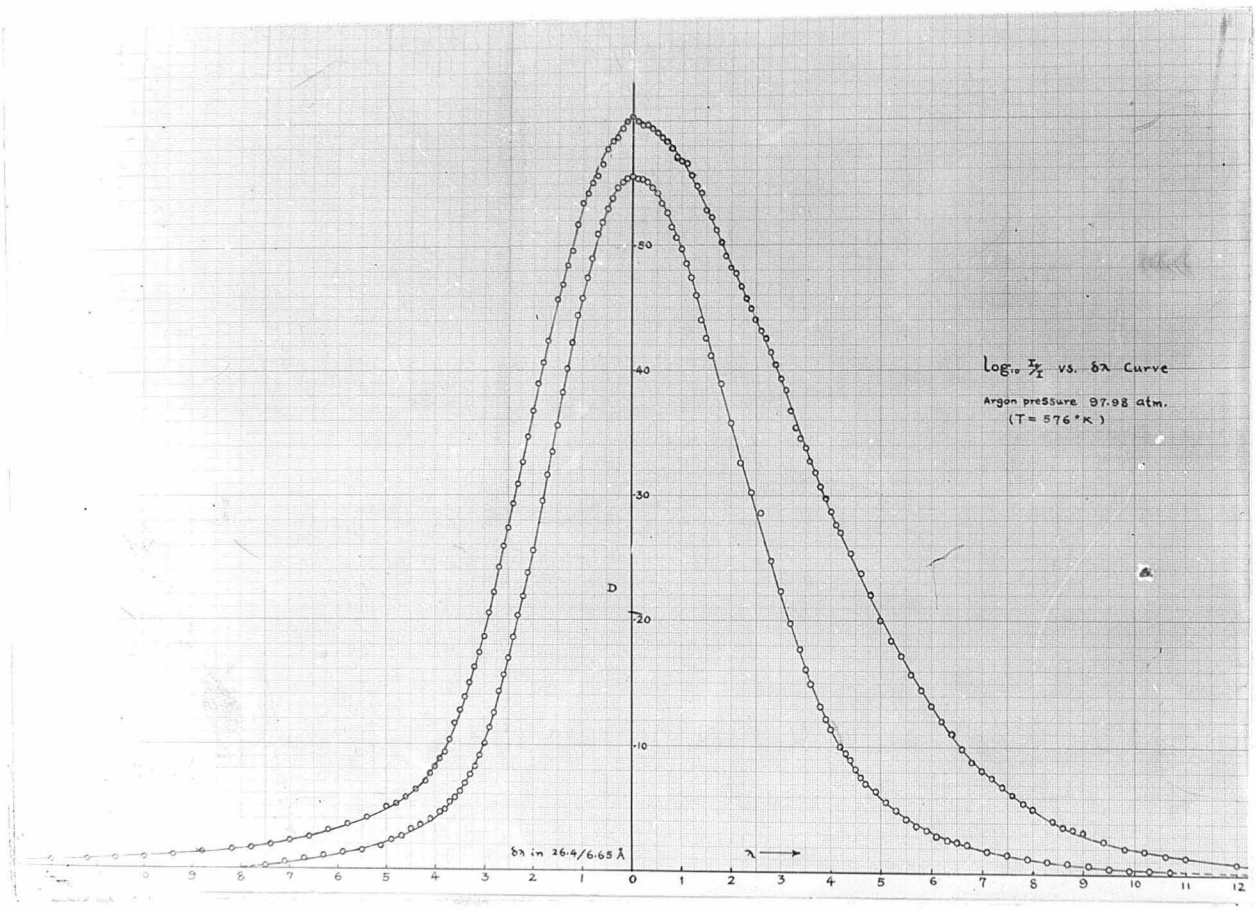
Log10 I/I vs. δλ Curve
Argon pressure 97.98 atm.
(T = 576°K)
D
.50
.40
.30
.20
.10
δλ in 26.4/6.65 Å
λ
9 8 7 6 5 4 3 2 1 0 1 2 3 4 5 6 7 8 9 10 11 12

Fig. 12 e.

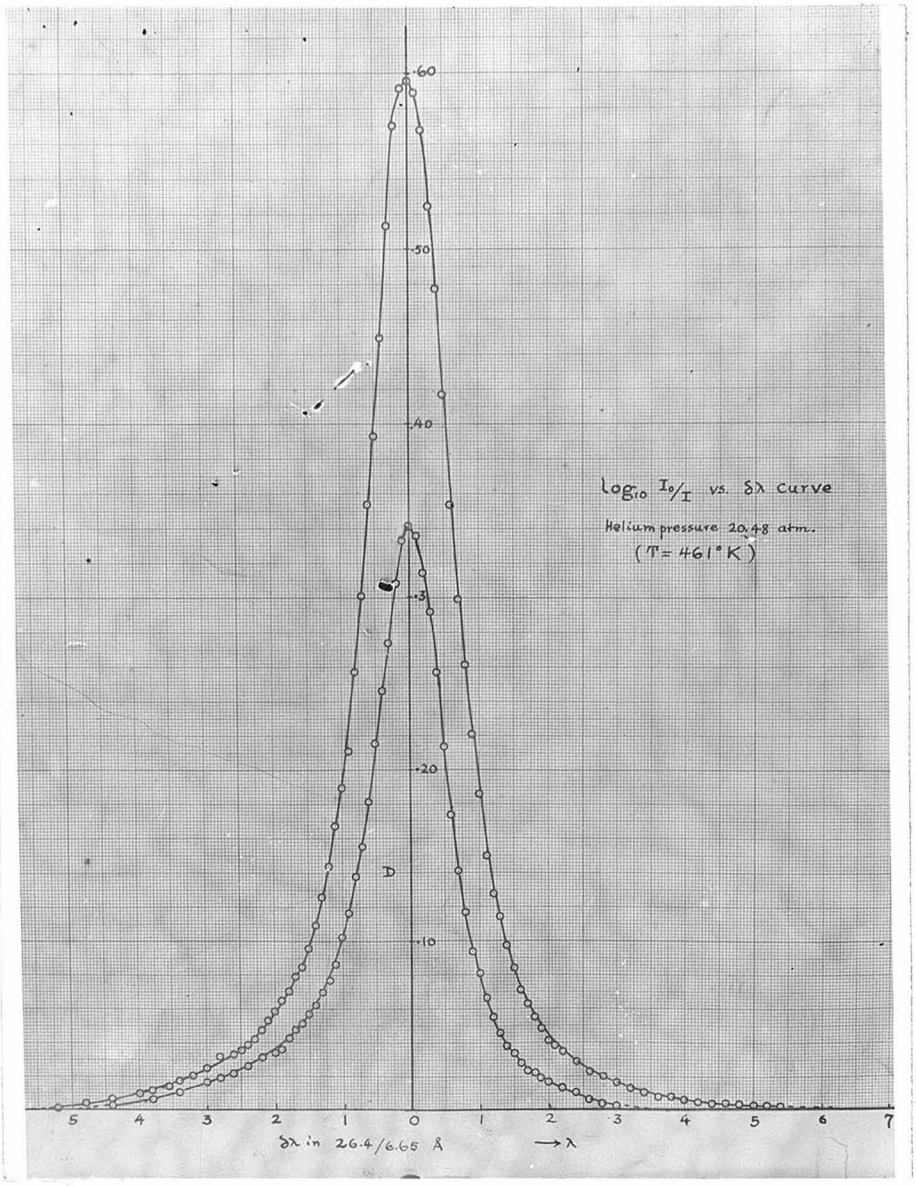
60
50
40
30
20
10
D
$\log_{10} I_0/I$ vs. δλ Curve
Helium pressure 20.48 atm.
(T = 461° K)
5 4 3 2 1 0 1 2 3 4 5 6 7
δλ in 26.4/6.65 Å
→λ

Fig. 12 f.

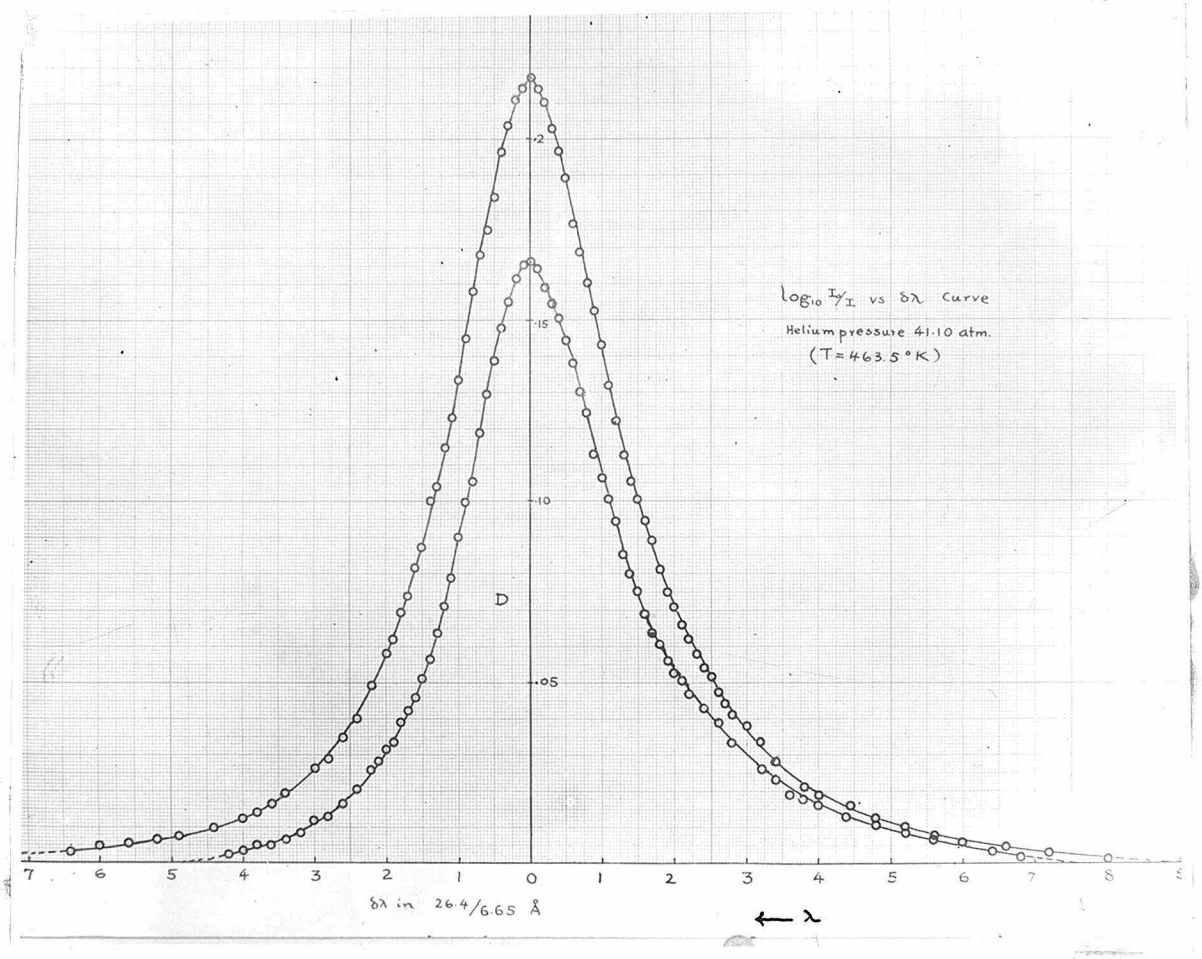
log10 Iy/I vs δλ curve
Helium pressure 41.10 atm.
(T = 463.5 °K)
·2
·15
·10
·05
D
7 6 5 4 3 2 1 0 1 2 3 4 5 6 7 8
δλ in 26.4/6.65 Å
← λ

Fig. 12 g

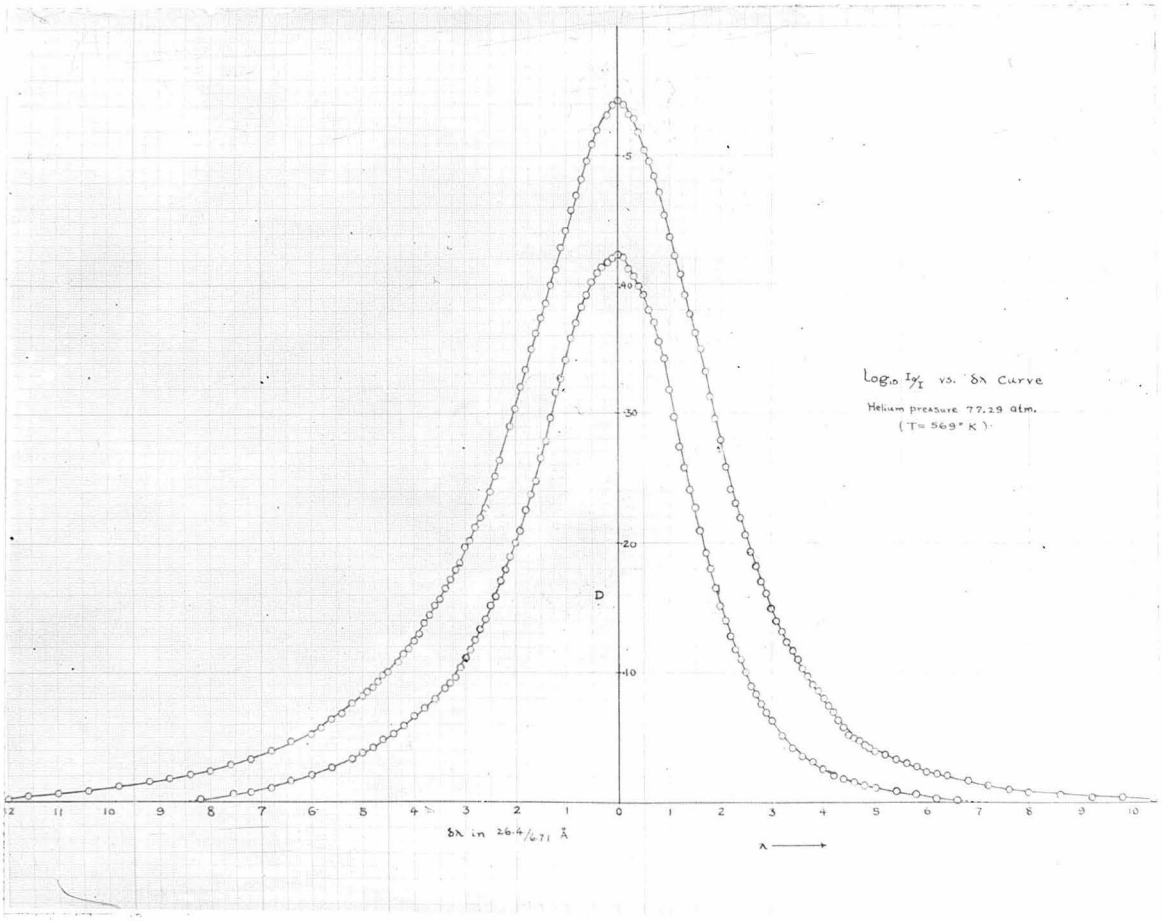
Log10 I0/I vs. δλ Curve
Helium pressure 77.29 atm.
(T= 569° K)
.5
.40
.30
.20
.10
D
12 11 10 9 8 7 6 5 4 3 2 1 0 1 2 3 4 5 6 7 8 9 10
δλ in 26.4/671 Å
λ

Fig. 12 h.

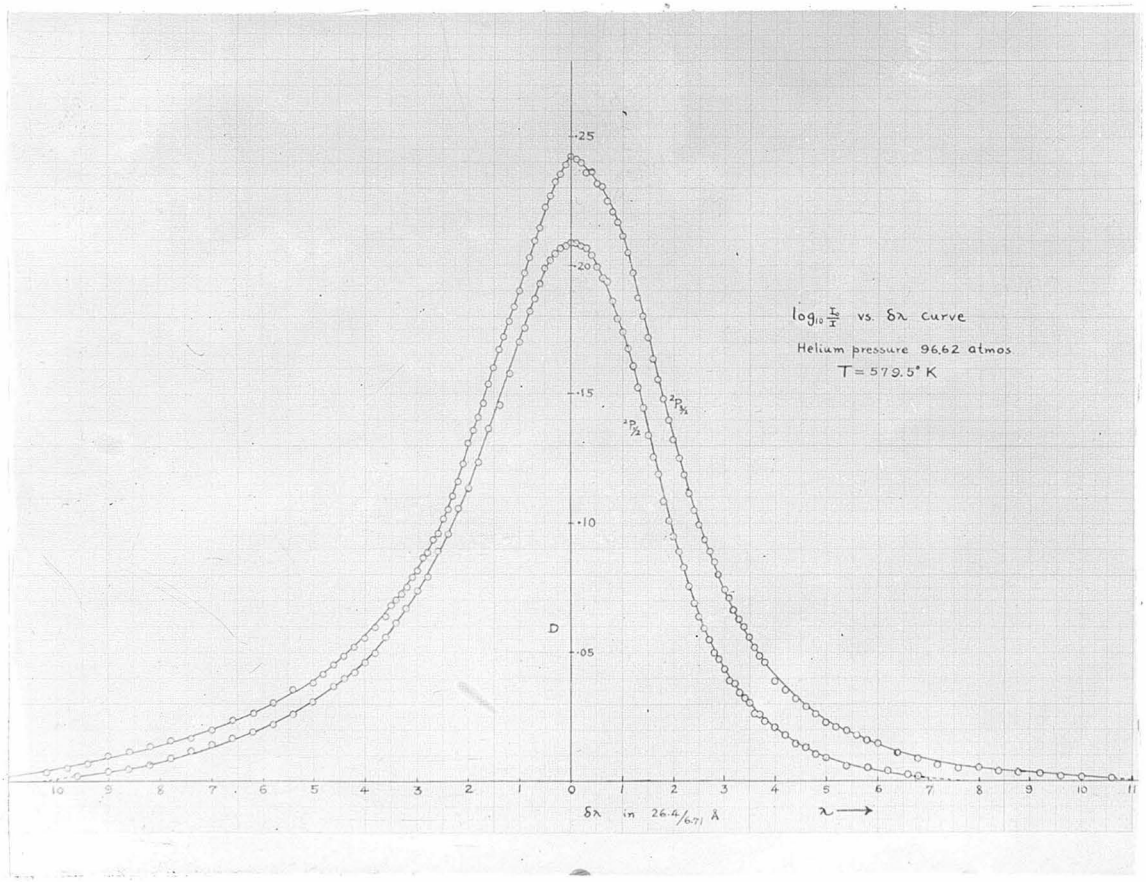
log10 I0/I vs. δλ curve
Helium pressure 96.62 atmos
T = 579.5° K
2P3/2
2P1/2
D
δλ in 26.4/6.71 Å
λ

Fig. 12 i

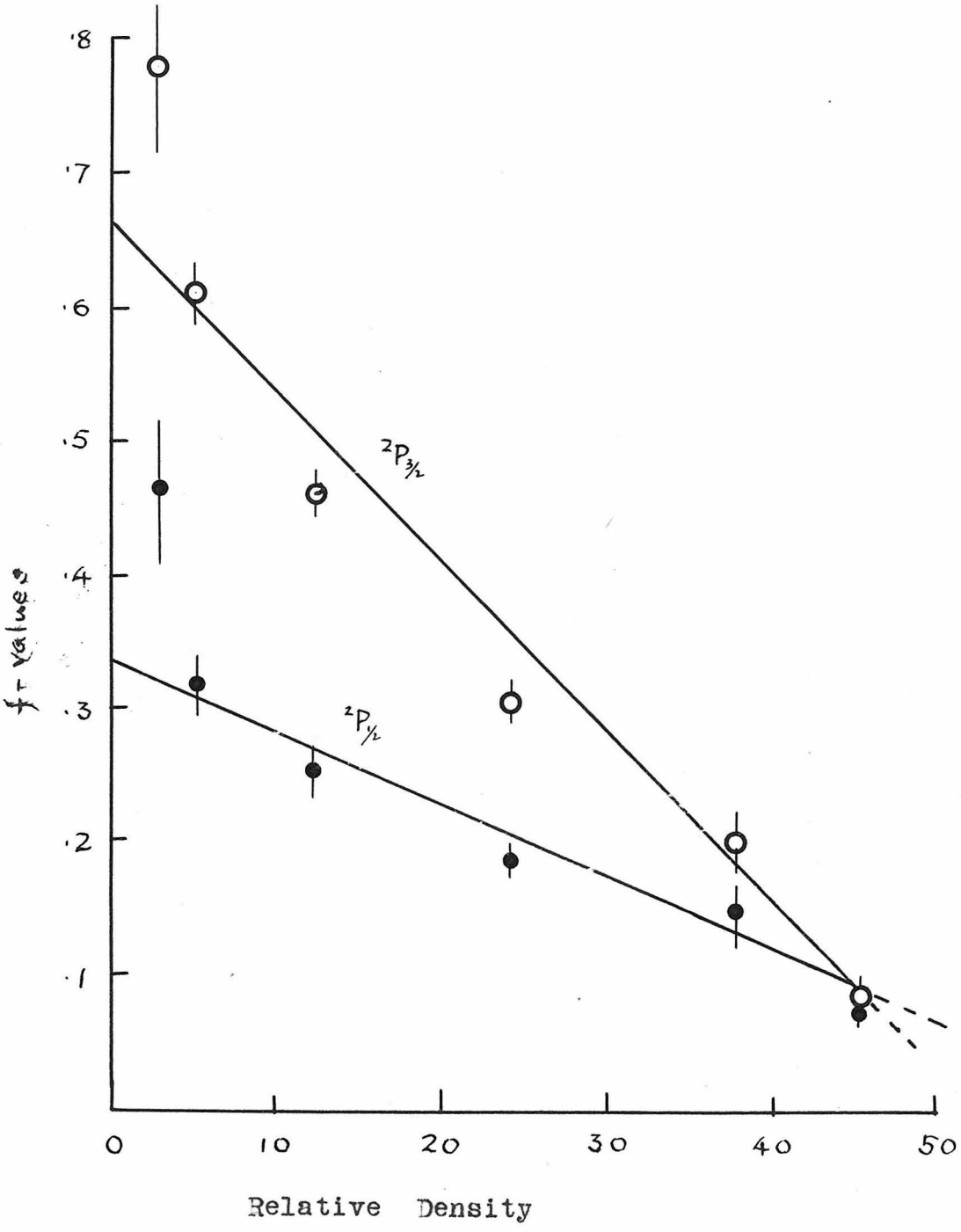

Fig. 13 f-value vs. relative density of helium

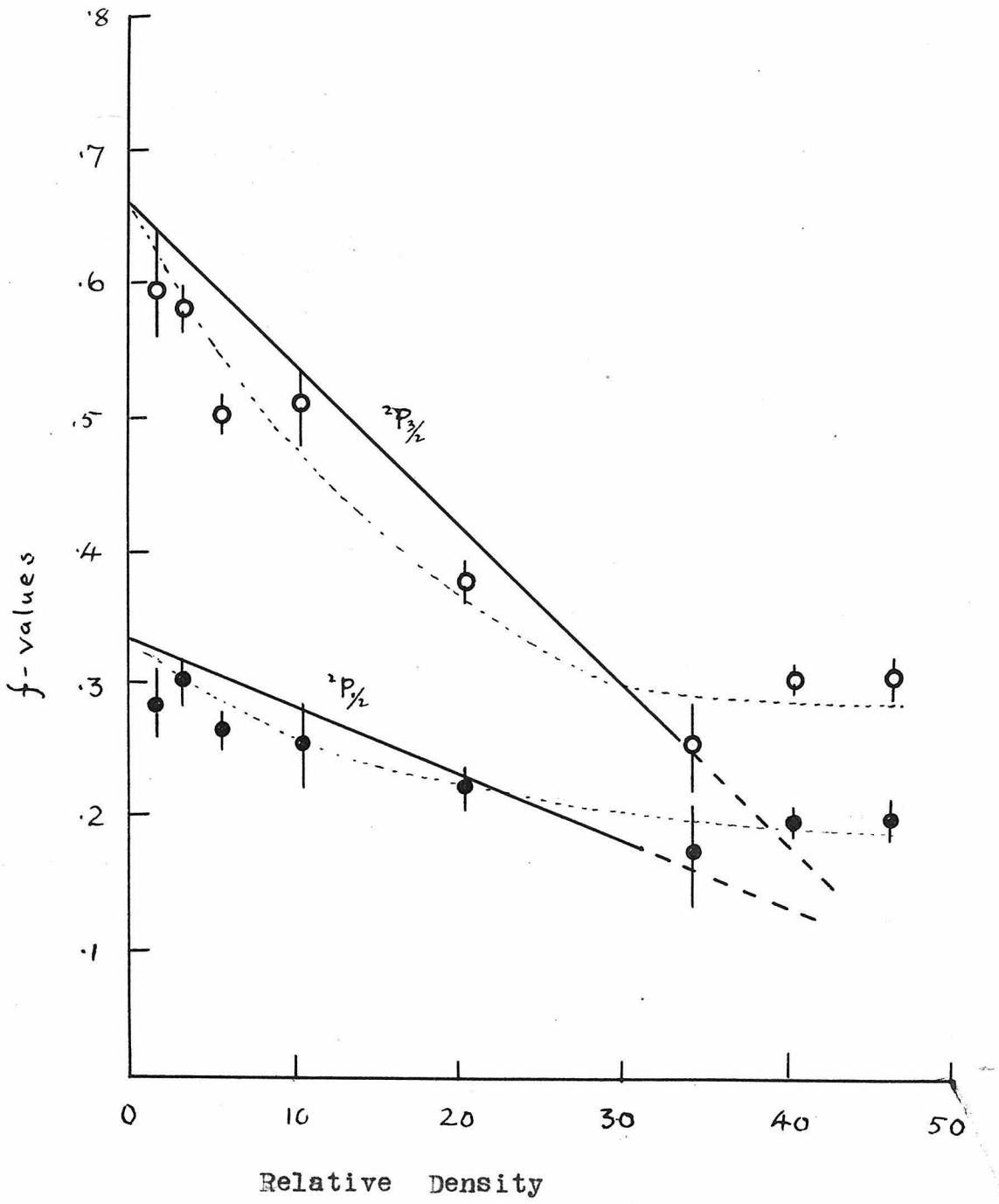

Fig. 14 f-value vs. relative density of argon

n = 2, and A= area under the line contour in cm^2.

From the amount of the total absorption, oscillator strengths and transition probabilities can be obtained. According to radiation theory the oscillator strength of the atoms, the f-values, is

$$f = \frac{4\nu m}{n e^2} \int_0^\infty (n\kappa)\ d\nu$$

and the transition probabilities, A_t

$$A_t = \frac{4\pi}{c n h} \int_0^\infty (n\kappa)\ d\nu$$
$$= (\pi e^2 / ch\nu m)\ f$$

The value of n can be found from equation (12) on page 18 of the preceeding article. Substituting the numerical constants

$$f = \frac{108}{22.75} \times 10^2 \frac{1}{\lambda n} \int_0^\infty (n\kappa)\ d\nu$$
$$= 6.086 \times 10^6\ 1/n \int_0^\infty (n\kappa)\ d\nu \qquad \text{for } \lambda 7800$$
$$= 5.974 \times 10^6\ 1/n \int_0^\infty (n\kappa)\ d\nu \qquad \text{for } \lambda 7947$$

and

$$A_t = 1.050 \times 10^{10}\ f \qquad \text{for } \lambda 7800$$
$$= 1.070 \times 10^{10}\ f \qquad \text{for } \lambda 7947$$

In Table V are listed the f-values when the lines were broadened by foreign gases. p and n stand for the vapor pressure and the concentration of the alkali vapor and R. D. the relative density of foreign gas. The f-values of the resonance lines without the presence of foreign gases were found by extrapolating to zero density of foreign gas as shown in Figs 13 and 14. The results are .33 and .66 for the $^2P_{\frac{1}{2}}$ and $^2P_{1\frac{1}{2}}$ components

respectively, and the corresponding transition probabilities are $6.93\ 10^9$ and $3.53\ 10^9$. These results agree with the results of Na, K and Cs resonance lines as measured by Minkowski, etc.[28].

As shown in Figs. 13 and 14 readings for low foreign gas concentrations were not so accurate owing to the inaccuracy in obtaining $\int_0^\infty (n\kappa)\, d\nu$. Also the readings for argon in Fig. 14 are not so good as those for helium. This might be due to the fact that argon was not so pure as helium; impurities such as oxygen would remove some alkali vapor causing a decrease in absorption. Great care was taken to heat the absorption tube for a long time after foreign gas was inserted, in order to be sure that the saturation of the alkali vapor in the absorption tube was recovered after the vapor being condensed by cold foreign gas or caught by impurity atoms.

---

(28) Minkowski, Z. f. Physik, 36 839, 1926
W. Schütz, ibid , 45, 30, 1927.
J. Weiler, ann. d. Physik, 1, 361, 1929.
Minkowski and Mühlenbruck, Z. f. Physik, 63, 198, 1930.
Weingeroff, ibid , 67, 679, 1931.
Ladenburg and Thiele, ibid , 72, 697, 1931.

(e) The optical collision diameters

The optical collision diameters can be computed from the observed line half widths.

$$\rho^2 = \frac{\pi \Delta\nu_{\frac{1}{2}}}{2\, n\, (2\pi k T)^{\frac{1}{2}}} \left(\frac{m M}{m + M}\right)^{\frac{1}{2}}$$

Where m and M are the masses of the absorbing and that of the perturbing atoms respectively.

Taking

$$\frac{\Delta\nu_{\frac{1}{2}}}{n} = .665 \text{ cm}^{-1}/\text{ r. d. for helium}$$

$$= .741 \text{ cm}^{-1}/\text{ r. d. for argon}$$

which are the mean values for the two doublet components. Then for argon and Rb

$$\rho^2 = \frac{3.14\ (.741)\ 3 \times 10^{10}}{2\ (2.7\times10^{19})\ (2\times3.14 \times 1.37 \times 10^{-16} \times 273)^{\frac{1}{2}}} \left(\frac{85.4\ (39.9)}{(85.4+39.9)\ 6.06\times10^{23}}\right)^{\frac{1}{2}}$$

$$\therefore \quad \rho = 13.37\ \text{Å}$$

While for helium and Rb

$$\rho^2 = \frac{3.14\ (.665)\ \times 3 \times 10^{10}}{2\ (2.7\times10^{19})\ (2\times3.14\times1.37\times10^{-16} \times 273)^{\frac{1}{2}}} \left(\frac{85.4\ (4.00)}{(85.44+4.00)\ 6.06\times10^{23}}\right)^{\frac{1}{2}}$$

$$\therefore \quad \rho = 7.75\ \text{Å}$$

Iv. Conclusion

A new absorption tube was constructed which made feasible the study of the broadening, asymmetry, and shift of rubidium resonance lines produced under different homogeneous pressures of pure helium and argon up to 100 atmospheres.

The lines exhibit velocity broadening even in this high pressure range as the half-width vs. relative density curves were linear. The broadening by argon is greater than that by helium and the broadening of the shorter wave-length component is slightly greater than that of the longer wave-length one for both gases. The difference between the half widths of the doublet components detected both by the author's former experiment on the second member of Rb principal series and by the present researches suggests again that the perturbing effect of neighbouring atoms (similar or dissimilar) may be different for different j-values.

Helium produces a violet while argon a red asymmetry. The degree of asymmetry increases as the concentration of foreign gas increases, and is greater for argon. For argon the asymmetry of the $^2P_{3/2}$ component is greater than that of the $^2P_{\frac{1}{2}}$ component while for helium the reverse is true. To describe the degree of asymmetry of the line contour by the ratios of the areas under the line contour is a more sensitive

way of measuring the asymmetry of the line than to describe it by the ratios of the red half to the violet half of the half-widths.

Argon produces a greater shift than helium. The former produces a strong red, while the later a violet shift. For both gases the shift of the $^2P_{\frac{1}{2}}$ component is greater than that of the $^2P_{1\frac{1}{2}}$ one. For helium the shift appears to be proportional to the relative density; while for argon the shift increases in general with the 3/2 power of the relative density. For argon the shifts for the doublet components are nearly the same, while for helium the shift of the longer wave-length component is about twice as great as that for the shorter wave-length component.

The areas under the absorption line contour($\log_{10}$ 1./1 vs.) for each line were measured. The f-values turn out to be .33 and .66 for the $^2P_{\frac{1}{2}}$ and $^2P_{1\frac{1}{2}}$ components of the Rb resonance lines respectively, and the corresponding transition probabilities are 6.93×10^9 and 3.53×10^9. The optical collision diameters estimated from the half-width data are 13.37 $^{o}_{A}$ for Rb-A and Rb-He respectively.

V. Acknowledgement

The author takes his great pleasure in expressing his gratitude to Prof. I.S. Bowen for his supervision and help throughout the research, and to Prof. W.V. Honston for his interest and encouragement. He also wishes to thank Mr. J.Pearson through his excellent technique and experience the absorption tube was made possible and to Mr. S.C. Lin for his help in completing many routine calculations.